I give permission for public access to my thesis and for copying to be done at the discretion of the archives' librarian and/or the College library.

__Kathryn Kinzel_____ ___May 14th, 2008__
Signature Date

FUNCTIONAL ANALYSIS OF INNER-ARM DYNEIN KNOCKDOWNS IN *TRYPANOSOMA BRUCEI*

by

Kathryn Whitney Kinzel

A Paper Presented to the

Faculty of Mount Holyoke College in

Partial Fulfillment of the Requirements for

the Degree of Bachelors of Arts with

Honor

Department of Biological Sciences

South Hadley, MA 01075

May, 2008

This paper was prepared
under the direction of
Professor Amy Springer
for eight credits

ACKNOWLEDGMENTS

First and foremost, I would like to thank Professor Amy Springer for taking me on as a research student, and for showing me how to be an effective scientist without going crazy. Your tremendous effort and guidance throughout the last year are greatly appreciated.

In addition, I would like to thank the Springer lab for all of their hard work - in particular, Sonia Dantas and Lindsey Poole for being thesis buddies, Tenaya Vallery, my fantastic lab monkey with sedimentation assays and other experiments, and Danielle Morgulis, my radio buddy and trouble maker for the longer experiments. Thanks also to Noël Rosenthal, for creating the building blocks that this work grew from.

A special thanks to Kate Plass, for being one of the best friends I could ever dream of having, and for being willing to proofread this thesis repeatedly (and leaving interesting comments) to make sure I was speaking English most of the time.

Thanks go out to Professor Sharon Stranford, for being my first introduction into research and for the generous use of her lab space; Marian Rice, for her expertise in all things microscopy; and Professor Amy Frary, for giving excellent advice as my adviser and thesis committee member.

A huge thank you to Professor Michele Klingbeil and her lab at UMass Amherst for the more than generous use of their lab, assistance with cloning and DAPI staining, and being able to sit on the thesis committee.

Thanks to Katherine Ralston in Kent Hill's lab at UCLA for sending protocols and assisting via email with sedimentation assays and TEM preparation.

Thanks to the Biology Department and to the Dreyfus Foundation for providing funding for this research and allowing me to present this work at conference.

I would also like to acknowledge the Medical Emergency Response Team, for helping me define an important part of who I am. In addition, a thanks to Kevin Fournier, Terry Fagnant, Kellie Cournoyer-Cronk, James Broussard, James Sullivan, Juan Rivera, Megan Smith, Jeffrey Baeder, Frank Rogala, Michelle Papineau, and the rest of the Department of Public Safety for keeping me grounded and well caffeinated, and for the near countless hours I have served with them.

A special thanks to Priyanjali Ghosh and Elena Puig, for keeping me sane and more or less on track, and for always listening to the latest rant about life.

Last, but certainly not least, a giant thank you to all of my friends for putting up with me and being there for me, and to my family, particularly my parents, for their everlasting love and support for all of my endeavors.

TABLE OF CONTENTS

LIST OF FIGURES

LIST OF TABLES

ABSTRACT

African Trypanosomasis is an endemic disease in sub-Saharan Africa caused by infection with the *Trypanosoma brucei* parasite. These unicellular eukaryotic organisms rely heavily on their single flagellum for movement and proliferation. Inside the flagellum, nine outer doublet microtubules surround a central microtubule pair in a structure called the axoneme; movement of the flagellum is dictated by the function of protein complexes called dyneins, which lie between the microtubules of the axoneme. These dyneins act as molecular motors by pushing the microtubules past each other, creating the flagellar beat and waveform.

There are several different types of proteins within the dynein complex and two different dynein types within the axoneme. This study looked at two genes believed to encode proteins in the inner-arm dynein: TbDNAH10, the putative inner-arm heavy chain alpha protein, and TbIC95, a probable intermediate chain.

In order to analyze the function of these gene products, the genes were individually knocked down using RNA interference, and cells were analyzed for motility, division, and morphological defects. TbDNAH10 knockdowns displayed a severe motility defect and had visible cell division defects. The TbIC95 knockdowns displayed a less severe but still noticeable motility defect, and managed to sustain better proliferation than the TbDNAH10 knockdowns. The results obtained suggest that these genes encode proteins essential for the inner-arm dyneins, and that these dyneins are essential for proper movement of the flagellum.

INTRODUCTION

Human African Trypanosomiasis

African Trypanosomiasis is a serious disease endemic in sub-Saharian Africa, killing thousands of humans and domesticated animals each year. The disease initially presents with symptoms common to many illnesses: fever, joint pain, and overall malaise (Centers for Disease Control 2004). As the disease progresses, infected persons begin to have neurological symptoms, including personality changes and alterations in circadian rhythms: patients sleep through the day and are awake at night. As the disease progresses, patients lapse into a coma, which is usually followed by death. The sleep changes and coma give the disease its colloquial name of "African Sleeping Sickness". Thirty-six countries in Africa are affected by this disease, with a reported incidence of 25,000-40,000 people contracting the disease each year (Centers for Disease Control 2004). The World Health Organization believes this to be a conservative number, and estimates the actual incidence rate to be closer to 100,000 people per year (World Health Organization 2006).

The disease is caused by the parasite *Trypanosoma brucei*, which is transmitted to humans through the bite of an infected tsetse fly. There are two subspecies of *T. brucei* that cause illness in humans: *T. brucei rhodesiense* and *T. brucei gambiense*. A third subspecies, *T. brucei brucei*, causes illness in cattle and other livestock. *T.b. rhodesiense* and *T.b. gambiense* are similar in nature but

are classified based on differences in disease progression. As a result, the disease is classified based on geographical region into East African Trypanosomiasis (*T.b. rhodesiense*) and West African Trypanosomiasis (*T.b. gambiense*) (Centers for Disease Control 2004) (Figure 1). East African Trypanosomiasis is more virulent but has a more limited range, whereas West African Trypanosomiasis is a more passive infection, creating a chronic condition that may not be detected right away. With both types of infections, initial symptoms are a result of the parasite within the bloodstream; later symptoms are caused by the parasite traveling to the brain via cerebrospinal fluid. It is currently unknown how the parasite is able to travel through the blood-brain barrier (Stich, Abel, and Krishna 2002).

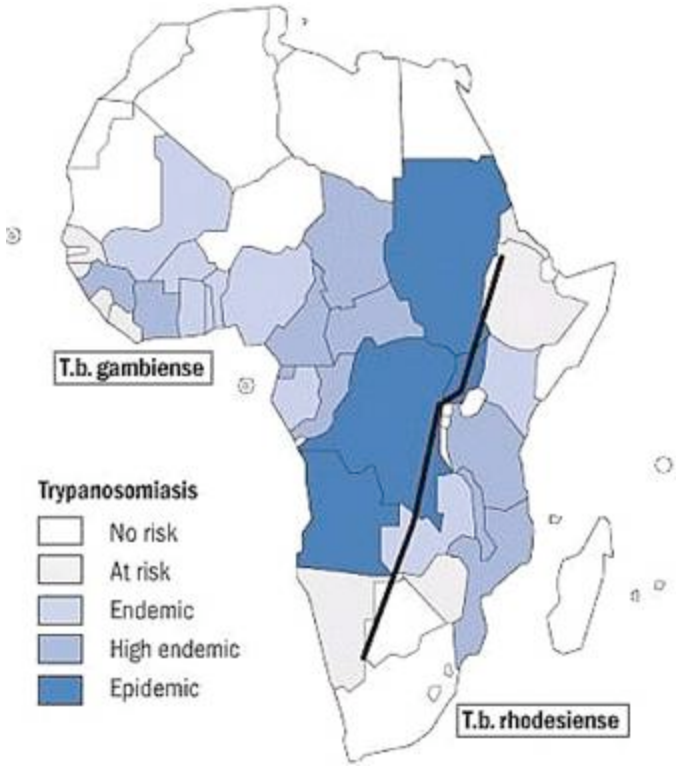

Figure 1 – Distribution patterns of *T. brucei gambiense* and *T. brucei rhodesiense*. The black line in the center of the picture shows the rough boundry between the two strains. The majority of countries south of the Sahara in Africa are at high risk of trypanosomiasis. From the Centers for Disease Control, 2004.

Treatment for the bloodborne parasite stage of the disease, while difficult, is possible with a high rate of success. Treatment after the parasite has traveled to the central nervous system is more invasive and deadly. It is difficult to get medication across the blood-brain barrier and attack only parasitic cells while leaving the rest of the brain relatively intact (Kennedy 2004). In 1905, Drs. H.W. Thomas and A. Breinl discovered the first effective treatment, Atoxyl. Though effective, Atoxyl contained arsenic at levels that were highly toxic and frequently

resulted in blindness (Pearce 1921). Over one hundred years later, the standard treatment for CNS trypanosomiasis is melarsoprol, another arsenic containing compound. Fatality rates from the drug alone reach 10%, and those who survive the treatment often have severe neurologic deficits (Kennedy 2004). Most of the deaths from the drug are a result of encephalopathy, brain damage as a result of increased intracranial pressure. However, the disease is 100% fatal if not treated, so even though there is an unacceptable risk of death by treatment, it is still less lethal than the death sentence the disease carries. In some areas of Africa, drug resistance with both strains of infectious *T. brucei* is becoming a problem, with up to 30% of new cases reported to have some melarsoprol resistance. A secondary treatment for the CNS form of the disease, eflornithine, has shown promise in being as effective and 25 times less deadly than melarsoprol (Chappuis et al. 2005). However, pharmaceutical companies do not find production of eflornithine to be cost effective, leading to limited supplies and inflated prices (Stich, Abel, and Krishna 2002). New treatments are desperately needed, and researchers are turning to the parasite itself to find novel drug targets and treatment options.

Trypanosoma brucei:

Trypanosoma brucei is a single-celled eukaryotic organism, relying on both human and tsetse fly for reproduction and transmission. This lifecycle is shown in Figure 2.

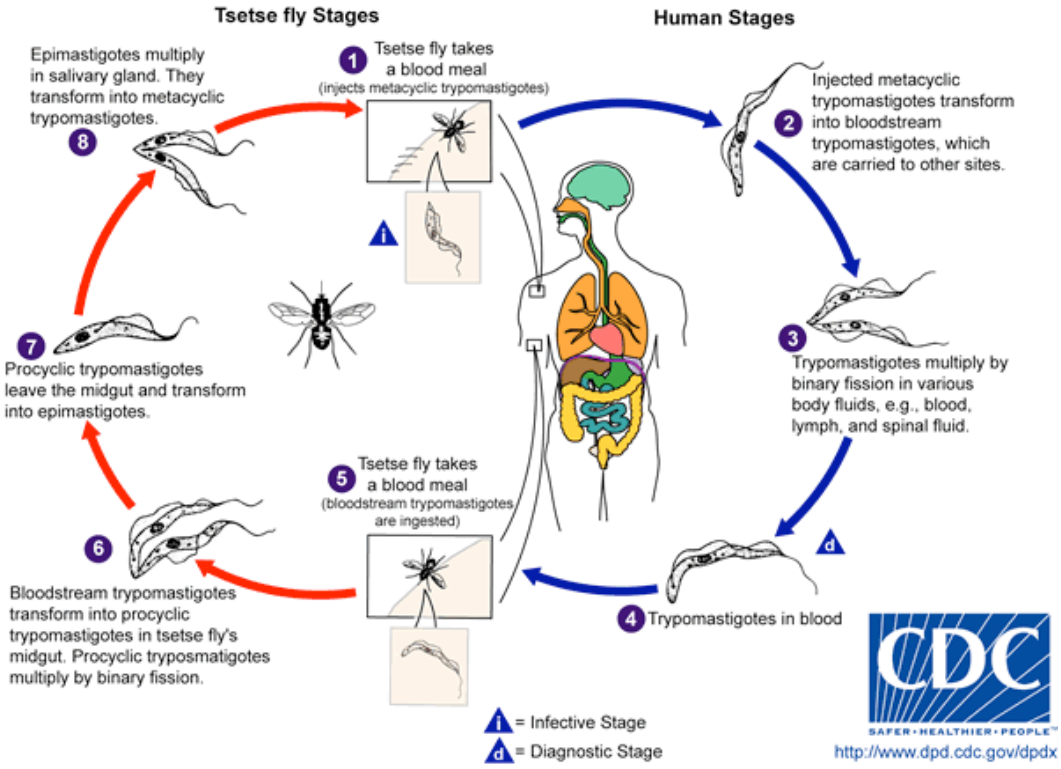

Figure 2 – Life cycle of *Trypanosoma brucei*. The parasite relies on both the human or mammalian host and the tsetse fly for replication and proliferation. Human infection begins at step one, with the injection of metacyclic cells into the host. The parasite changes into its bloodstream form and undergoes division in steps two through four before being taken up in a blood meal at step five. The bloodstream trypomastigotes then transform into procyclic trypomastigotes, where they undergo further divisions (step six) and travel to the salivary glands of the fly (step seven) where they transform into their metacyclic form (step eight) and are ready to infect the next host. From the Centers for Disease Control, 2004.

Tsetse flies become infected upon taking a blood meal from an infected mammal (Fig. 2, Step 5). Trypanosomes present in the blood attach to the wall of the midgut in the fly, where they transform into procyclic trypomastigotes (Fig. 2, Step 6). These procyclics undergo a growth phase before transforming into epimastigotes, which leave the midgut and travel to the salivary glands via an unknown process (Fig. 2, Step 7). Once in the salivary gland, the epimastigotes multiply and transform into metacyclic trypomastigotes, which allows the parasite to be transmitted to a mammalian host on the fly's next blood meal (Fig. 2, Step 1) (Kennedy 2004). Once inside the mammalian host, the trypanosomes transform into bloodstream trypomastigotes, where they travel to different parts of the body and replicate further (Fig. 2, Steps 2-3). These bloodstream trypomastigotes can be taken up by another tsetse fly, thus continuing the lifecycle. Completion of the cycle allows for trypanosomes to continue to spread and infect humans and livestock - likewise, the prevalence of disease allows for spread by tsetse fly. Arresting the cycle at any step effectively halts the spread of both trypanosome and disease.

The cell structure of *T. brucei* is like many eukaryotic organisms, with a few interesting differences many of which are related to the flagellum of the cell. There is one large mitochondrion in the cell, which has an unusual direct attachment to the basal body of the single flagellum. Mitochondria are usually attachment free and dispersed throughout the cell. As a result of the connection,

cellular division is linked to division of the mitochondrion and division of the basal body (Bastin et al. 2000). The external site of flagellar attachment, called the flagellar pocket, is the one site on the cell where exocytosis and endocytosis occur (Bastin et al 2000). Most other cells are able to exocytose and endocytose across the entire membrane, so having only one location on the cell where movement across the cell membrane can occur creates a very controlled regulation mechanism. The rest of the cell membrane is covered in proteins, called variable surface antigens. These proteins are coded by a series of genes in several loci, which results in different genes being expressed throughout the lifespan of the parasite (Donelson 2003). Depending on what gene is being expressed at any given time, the protein surface of the cell membrane will change and appear different over time. It is this changing outer surface that allows for the trypanosome to evade the immune system, and makes producing vaccines and other drug treatments difficult. Many drugs and all vaccines depend on having a standard, predictable surface for selective binding. A randomly varying surface that can change frequently makes it impossible to create a drug or vaccine with any selectivity, rendering those treatments completely ineffective (Donelson 2003).

Flagellar Structure:

One of the more interesting organelles of the trypanosome is the flagellum. The flagellum is wrapped around the cell, starting from the flagellar pocket on the posterior of the cell and extending out past the anterior of the cell (Vaughan and Gull 2003). This attachment is dictated by a group of proteins and microtubules within the membrane of the flagellum, called the flagellar attachment zone (Vaughan and Gull 2003). Like the rest of the trypanosomatid family, and unlike most other flagella, the flagellum in *T. brucei* begins beating from the outer tip, rather than from the base (Hill 2003). Most flagella use the solid connection at the base as a strong starting point for beat propagation; it initally seems counter-intuitive to rely on a small flagellar tip to provide the energy and physical movement required to start an effective flagellar wave propagation. However, it is effective: due to the position of initial beat formation and the location of the flagellum, the cell is pulled through its environment, with the body of the cell moving in an auger-like spiral shape due to the longitudinal attachment of the flagellum (Hill 2003) (Figure 3).

Figure 3 – Drawing of trypanosome swimming direction. The flagellum begins its motion from the tip, located on the right side of this image. In addition, the flagellum pulls the trypanosome instead of pushing it, and the flagellum is wrapped around the length of the cell. As a result, the flagellum pulls on the entire cell body, and movement is in a spiral shape towards its tip, as shown with the red line. From Hill, 2003.

A large, electron-dense protein structure called the paraflagellar rod (PFR) is enclosed within the flagellum's membrane, and runs parallel with the flagellum (Bastin et al. 1999). The function of the PFR is still unknown, although current hypotheses suggest that the PFR stabilizes the flagellum as it beats, aiding the forces acting on the attached flagellum, and one new study proposes that the PFR is a site of energy metabolism (Pullen et al. 2004).

The flagellum contains a highly conserved structure called the axoneme (Figure 4). The axoneme is composed of nine doublet microtubules arranged in a circle, surrounding a pair of microtubules in the center. All motile flagella and cilia have this "9+2" arrangement; non-motile flagella and cilia usually have a "9+0" arrangement, with the central pair missing (Bastin et al. 2000). Numerous

proteins are located within the axoneme, providing both structural and functional support (Dutcher 1995).

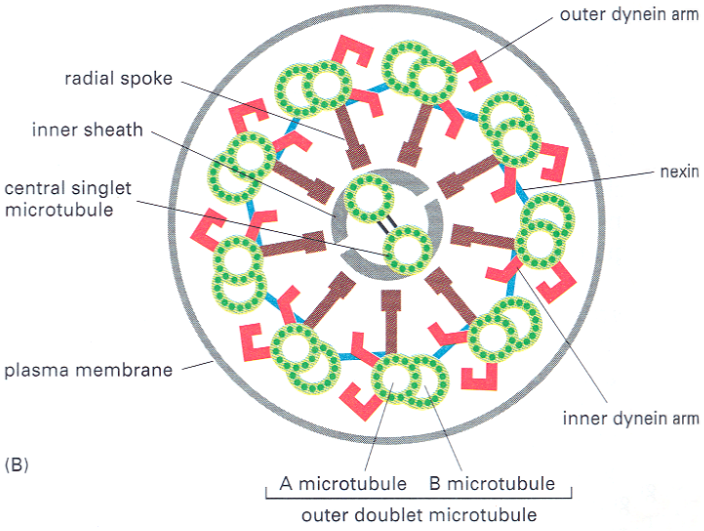

Figure 4 – Cartoon of the 9 + 2 axoneme structure. Microtubules are colored in green, with the nine doublet microtubules surrounding the central pair. Nexin links (blue) connect the outer microtubules to each other and keep them from sliding past each other. Radial spokes (brown) provide connections between the doublet microtubules and the central pair. Dyneins (red) are the motors that create microtubule movement. There are two types of dyneins within the axoneme - outer-arm dyneins and inner-arm dyneins, named for their location on the doublet microtubules. From Alberts et al, 2002.

In other locations in the cell, when microtubules are pushed against each other, they are able to freely slide in opposite directions (Gibbons 1988) (Figure 5). However, in the flagellum, protein links called nexins connect the microtubules together. The microtubules are unable to slide away from each other, so a bend is produced instead. It is this coordinated bending motion that

causes the periodical motion of the flagellum and allows for propulsion of the cell (Gibbons 1988).

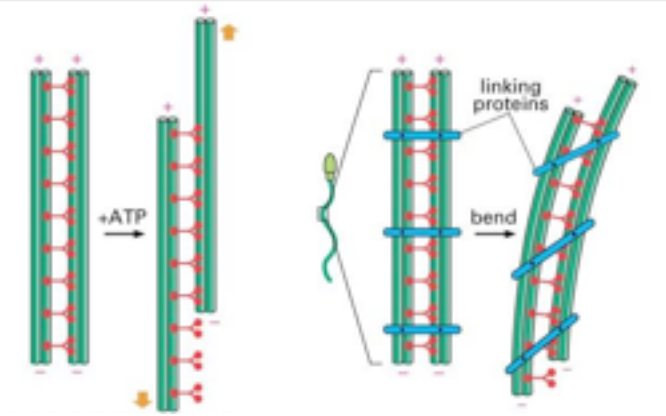

Figure 5 – Cartoon of microtubule movement. When both microtubules are free, a sliding motion occurs. However, when the microtubules are bound to each other, as in the case of flagella, a bending motion is produced when the microtubules try to slide away from each other. From Alberts et al, 2002.

Several proteins provide support for this bending, including radial spokes from the doublet microtubules to the central pair, and sheath-like proteins that encapsulate the central pair (Baron et al. 2007; Bastin et al. 2000). However, the cell is unable to move if the flagellum is unable to bend. The flagellum thus relies on protein motors, called dyneins, to provide this movement.

Dyneins

Dyneins are the complexes that drive the movement of the flagellum through microtubule bending. These molecular motors are composed of several different proteins in a large complex in contact with the microtubule. Hydrolysis of ATP leads to a structural change in the dynein, moving the “head” forward

along the microtubule with a slight twisting motion (Burgess and Knight 2004) (Figure 6).

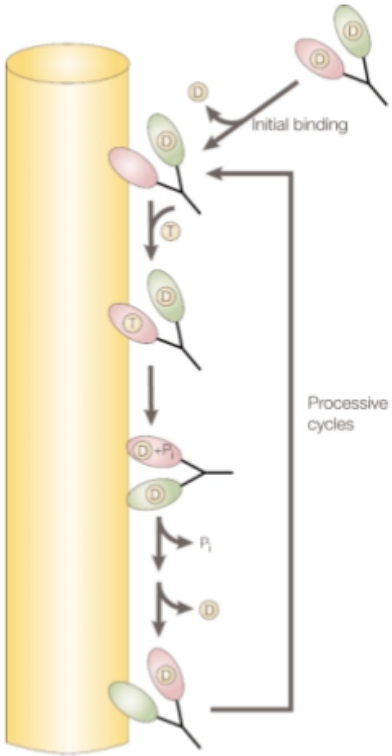

Figure 6 – Cartoon of motor "walking" on microtubule. This image shows the systematic binding and releasing of the heads of the motor proteins, in this case, kinesin. Initial binding takes place with the release of ADP, and subsequent hydrolysis of ATP results in a conformational change in the protein, bringing the second head into proximity to the microtubule. The process then repeats. From Woehlke and Schliwa, 2000.

Dyneins always travel towards the negative end of the microtubule, which is located in the base of the flagellum (Gibbons 1988). Within the axoneme, there are two types of dynein: outer-arm dyneins and inner-arm dyneins (Dutcher 1995). The names for the dyneins reflect their relative position in the flagellum: outer-arm dyneins are located on the periphery of the doublet microtubules, whereas the inner-arm dyneins are on the side facing the central pair (see Figure 4). The dyneins are connected to adjacent microtubules, allowing for specific

bending on one part of the flagellum at a time (Gibbons 1988). Outer-arm dyneins are smaller and occur every 24nm on the microtubules. Inner-arm dyneins are comparatively more complex and occur every 96nm along the length of the axoneme (Figure 7) (Nicastro et al. 2006).

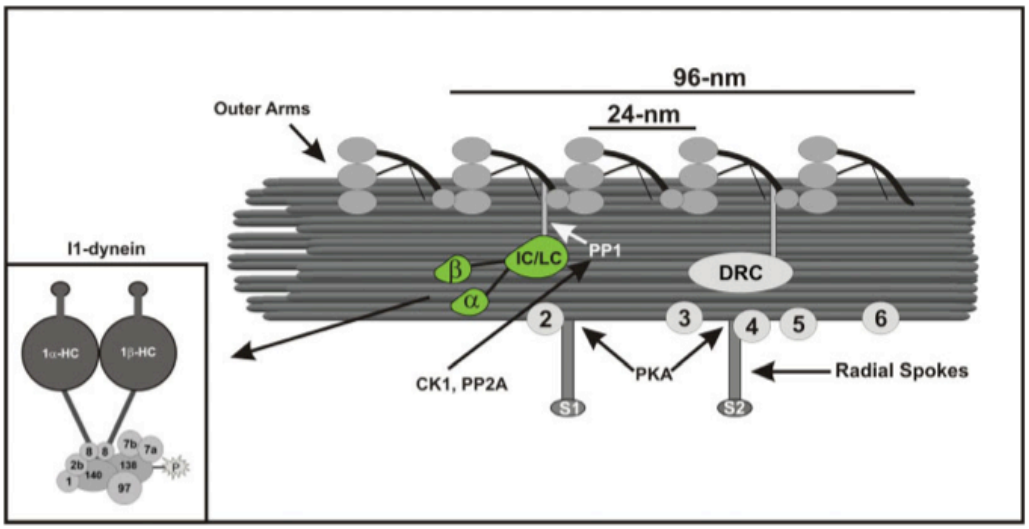

Figure 7 – Longitudinal cartoon of dyneins on a microtubule. Outer-arm dyneins repeat their structure every 24 nanometers, compared to the inner-arm dyneins that repeat every 96 nanometers. The area highlighted in green is the traditional "motor" part of the inner-arm dynein (insert), however the entirety of the dynein includes the proteins marked 2-6. From Wirschell et al, 2007.

Both dyneins have at least one protein unit that is classified into one of three categories: heavy, intermediate, and light chains. Outer and inner dynein arms have different numbers of polypeptide chains; however many of these protein units share similarity across species, which suggests that the function of the dynein relies on the overall shape of the protein complex (Dutcher 1995).

Previous studies

Previous studies have shown that proper assembly of components of the flagellum are necessary for functional motility, and most of these proteins have been a part of the central pair or radial spoke protein complexes (see Figure 4) (Baron, Kabututu, and Hill 2007; Bastin et al. 1999; Branche et al. 2006; Ralston and Hill 2006). Kent Hill and his lab found several proteins within the axoneme that are "components of motile flagella", which are found in organisms with motile flagella and not in organisms with immotile flagella. With many of these proteins, it was demonstrated that the absence of the protein transcript would lead to some loss of motility, showing that the protein was required for motility. The amount of motility lost would vary by protein, but nearly all exhibited some motility defect, showing that the proteins were required for proper flagellar movement (Baron et al. 2007). With regards to the dynein complexes, it has been suggested that the components of the dynein must be present for proper assembly to occur, where a lack of one protein may destabilize the protein complex enough to result in misassembly (Myster et al. 1999). In addition, proper motility in the trypanosome is required for the bloodstream form of the cell to undergo successful cytokinesis, an unusual trait that is not normally seen in flagellated cells (Broadhead et al. 2006).

This Research

This study focuses on two genes that we currently refer to as TbDNAH10 and TbIC95. TbDNAH10 is believed to encode for a 1-alpha heavy chain (1-alphaHC) arm in the inner-arm dynein. This gene has 44% amino acid identity to the heavy chain 10 dynein arm in humans, and has coding characteristics typical to DHC sequences, including six ATP binding regions and a microtubule binding region (Burgess and Knight 2004). In *Chlamydomonas*, a biflagellated alga that is frequently used as a model system for flagellar structure and function, a homologue mutant of this gene had a noticeable defect in flagellum function, but it was not as severe as other mutants being studied. TbIC95 is believed to encode for an intermediate chain protein within the inner-arm dynein. A protein with similar sequence, IC138, has been studied in *Chlamydomonas* and has been shown to have an important role in flagellar bending (Hendrickson et al. 2004). TbIC95 shares roughly 33% amino acid identity to IC138, with the most similarity in a WD-repeat heavy region, a sequence that is common in this type of dynein protein. It is currently unknown if either TbDNAH10 or TbIC95 are the *T. brucei* homologues to 1-alphaHC or IC138 respectively, or if these proteins share similar roles to their possible homologues within the dynein.

TbDNAH10 and TbIC95 were selectively knocked down using inducible RNA interference (RNAi) in order to characterize the motility defects and to elucidate the probable role of these predicted proteins in *T. brucei* flagellar

movement. RNAi is a relatively new process which allows for selective knockdowns of gene products by interfering with messenger RNA with small interfering RNAs. These siRNAs create double stranded RNA, which the cell is able to recognize and specifically destroy (Mello and Conte 2004). Using the same apparatus, the cell then destroys all RNA with the same sequence as the siRNAs, destroying the normal mRNA and effectively stopping that protein's production. With RNAi, it is possible to keep the trypanosome genome intact and induce the mutation repeatedly and at will. Plasmids containing a section of either TbDNAH10 or TbIC95 were transfected into *T. brucei brucei* trypanosomes, and the transfected cell lines were renamed DNAH10i and IC95i respectively. Both of these cell lines showed a motility defect upon RNAi induction, demonstrating the requirement of these proteins in motile flagella.

Trypanosome motility is vital in its lifecycle, so an understanding of the mechanisms by which the trypanosomes can travel and infect can potentially provide for new drug targets, which could make new treatments available for thousands of people across the world. In addition, because the structure of the axoneme and enclosed proteins is so highly conserved across all eukaryotic organisms, elucidating function of a component in one organism allows for similar conclusions to be made in other organisms. Flagellar studies are much easier to conduct in single-cellular organisms like *T. brucei*, and yet many of the proteins within the flagellum have the same function in different organisms'

flagella. Several human diseases are a result of misfunctioning flagella and cilia, and so by gaining a better understanding of the functional components of motile flagella, treatments and cures for these diseases could be created. By focusing this work on the important dynein motors, insight into the mechanisms of flagllar movement can begin to be worked out, providing valuable information on the molecular level that can be extrapolated across species and across diseases.

MATERIALS AND METHODS

Cell Culturing

All cell culturing was performed in a laminar flow hood with biosafety level two precautions. *T. brucei brucei* was used due to its inability to infect humans.

Complete medium was made by adding 2mg/mL sodium bicarbonate to SDM-79 pre-mix (SAFC/Sigma, http://www.sigmaaldrich.com), adjusting pH to 7.4, and adding 3µL of hemin and 180µL sterile Fetal Bovine Serum (heat-inactivated, "premium" from Biomeda, http://www.biomeda.com or "characterized" from HyClone of Thermo Fisher Scientific, http:// www.hyclone.com) for every 1mL of medium. Added to the complete medium were three antibiotics purchased from MP Biomedicals (http://www.mpbio.com) or Thermo Fisher Scientific Inc. (http://www.fishersci.com): G418 to 15µg/mL, Hygromycin to 50µg/mL, and Phleomycin to 2.5µg/mL. These drugs were either added directly to the medium or were added to the cultures when medium was added. Conditioned medium was created by mixing one volume of filtered spent medium with one volume of fresh complete medium and 0.4 volumes of FBS.

Cell lines were periodically frozen for future use. Cells at 5-6 * 10^6 were put into 800µL aliquots in cryovials with 200µL of sterile 50% glycerol. The cryovials were then frozen at -80˚C overnight and transferred to liquid nitrogen after 24 hours. Frozen cells were thawed slowly, diluting 1:2 in complete medium for the first 24 hours, with one mL of medium added every 24 hours for three

days. Cultures were then passaged by diluting at least 1:10 every two to three days, making sure to keep cells between 2 * 10^5 and 1 * 10^7 cells/mL. Counting was conducted using a hemacytometer and a Nikon Eclipse TS100 inverted microscope (Nikon, http://www.nikon.com/products/instruments/index.htm). Passaging was done until the glycerol concentration was below 0.2% and stable growth was achieved.

For RNAi induction, cultures were divided into two flasks to allow for parallel growth, and Tetracycline to 1µg/mL was added to one flask.

Single-Cell Dilution Cloning

Cloning was conducted using the protocols established by the Klingbeil lab, UMass Amherst. Cultures growing at log phase (~5-7*10^6 cells/mL) were diluted to a concentration of one cell/mL in 20mL of conditioned medium and plated onto a 96 well plate. Plates were incubated at 27°C in the presence of CO_2 for approximately two weeks until turbidity was present. The contents from the well were then placed into a larger culture flask with fresh medium and grown as a regular culture for approximately one week. To ensure healthy growth, the cultures were diluted three times over the course of the week (see above). Cultures were then frozen in 1mL aliquots for future use as described above.

Growth Curves

Cell lines were split in parallel and induced, and the cell titer was determined every 24 hours for 120 hours. Cultures occasionally needed to be

diluted to keep cells at healthy concentrations, so cell titers were multiplied by these dilutions. This new titer is thus representative of how well the cultures were growing, and gives the number of total cells that would have been present with no diluting. Induced cultures were also placed in an incubator with continuous shaking at 80rpm. These data were then entered into Excel (Microsoft, http://www.microsoft.com) and plotted using a standard XY scatter plot.

Sedimentation Assays

Sedimentation assays were conducted following the protocols as explained in Ralston et al, 2006. 1.5mL of cell cultures (uninduced and 48 hours post-induction) at 5-6*10^6 cells/mL were placed into cuvettes, two cuvettes per culture. The optical density at 600nm was measured every two hours in a Beckman DU640 spectrophotometer (Beckman Coulter, http://www.beckmancoulter.com/) and prior to measurement one cuvette per culture was resuspended using a pipet. Cuvettes were kept in an incubator at 27°C in between measurements. Data were entered into Excel, where the difference between the resuspended culture and the undisturbed culture were determined and plotted using a standard XY scatter plot.

Time-Lapse Assays

Analysis followed protocols as explained in Baron et al, 2007. Cells at various time points post induction were observed in a hemacytometer using an inverted Nikon Eclipse TE2000-U microscope (Nikon, http://www.nikon.com/products/instruments/index.htm). Images of the cells were taken every second for

thirty seconds using a Roper Coolsnap HQ digital camera (Roper Scientific, http://www.roperscientific.de/coolsnap.html) and MetaVue Imaging software (Molecular Devices, http://www.moleculardevices.com/), and the resulting stack was made into a standard 1 frame per 1/30 seconds Quicktime movie (Apple, http://www.apple.com/quicktime). Screenshots were made of the starting frame of these movies, and individual trypanosomes (~200 for each time point) were observed for the length of the movie. Trypanosomes were then placed into one of three categories: Runner, Tumbler, and Immotile. "Runners" had a forward motion that lasted for more than five seconds, "Tumblers" moved but did not maintain a forward motion for five seconds, and instead moved in circles or brief motions, and "Immotile" cells did not have any cellular motion at all. Trypanosomes were monitored using the first frame of the movie using the image program Gimp (GNU General Public License, http://www.gimp.org) and image modifying features in Appleworks (Apple, http://www.apple.com). Trypanosome counts were taken from these images and placed and analyzed in Excel.

Fluorescence Microscopy

Microscopy was conducted following the protocol given by Klingbeil et al, 2002. One milliliter of cells growing at around 5-6*10^6 cells are collected, centrifuged and then washed and resuspended in 1mL PBS. Cells were then placed onto a poly-lysine coated slide and allowed to adhere for ~10 minutes in a humid chamber. Cells were then fixed with 4% paraformaldehyde for five

minutes at room temperature. Slide was then rinsed with PBS three times, five minutes each wash. DAPI was then placed on the slide at a concentration of 1µg/mL for 60 seconds, and the slide was washed twice with PBS for five minutes each wash. The slide was then mounted in Slow-Fade and cells were observed using an Olympus BH2 microscope (Olympus, http://www.olympusamerica.com/seg_section/seg_home.asp). Images were taken using an Olympus C5050 camera (Olympus, http://www.olympusamerica.com/cpg_section/cpg_digital_slr.asp). Picture resolution was adjusted to 300dpi and scale bars added using Adobe Photoshop Elements (Adobe, http://www.adobe.com/products/photoshopelwin/) and selections were cropped using ImageJ (NIH opensource, http://rsb.info.nih.gov/ij/).

Scanning Electron Microscopy

Protocol was based on the protocols of Sherman and Gull, 1989. $1*10^8$ cells were spun down and washed in PBS, and fixed in 4% paraformaldehyde at 4˚C overnight. Cells were then placed on coverslips coated with poly-L-lysine for 45 minutes in a humid chamber. Coverslips were rinsed with distilled water and mounted on aluminum stubs, and sputter coated with ~15nm of gold. Samples were viewed using a FEI scanning electron microscope (FEI, http://www.fei.com/). Individual pictures were taken with the microscope, and survey pictures were modified with Adobe Photoshop Elements. The measurement of

clumped cells was obtained by counting the number of clumps present in fifty random fields.

Transmission Electron Microscopy

Cytoskeleton extraction was conducted following protocols from the Hill lab, UCLA. $2*10^8$ cells were washed three times with PBS and resuspended in PEME buffer with 1% TritonX. After a five-minute incubation, cells were washed once with PEME before continuing to regular transmission electron microscopy preparation.

Regular preparation: Cells were fixed in a 0.1M sodium cacodylate solution containing 2.5% glutaraldehyde, and 1% tannic acid for one hour. After a cacodylate wash, cells were post-fixed with 1% osmium tetroxide and 1.5% potassium ferricyanide for one hour. The cells were then placed in a low-melt agarose cube, dehydrated through an ethanol series, and infiltrated with Spurr's resin, average hardness. Samples were then embedded in Spurr's at 70°C for 24 hours. Samples were thin sectioned and stained in lead citrate and uranyl acetate by Marian Rice, Mount Holyoke College. Samples were viewed using a Philips C150 TEM (Philips, http://www.usa.philips.com).

RESULTS

DNAH10i and IC95i induced cells grow slower

Growth curves are shown in Figure 8 for DNAH10i, Figure 9 for IC95i-C5, and Figure 10 for IC95i-F9. As shown in each, the induced cells grew more slowly than the uninduced cells. DNAH10i induced cells showed a noticeable difference in growth rates after 24 hours post-induction, and were not able to regain any semblance of normal growth.

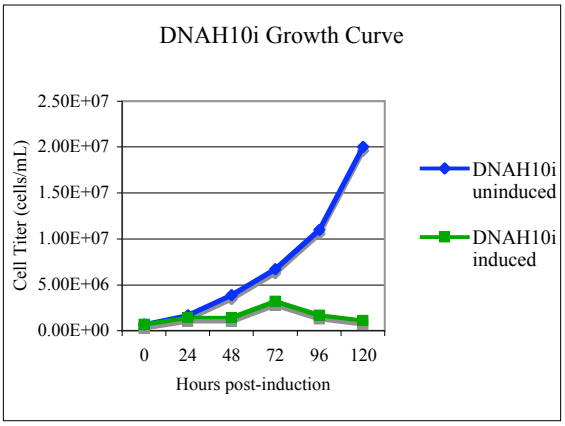

Figure 8 – DNAH10i growth curve. Cell titers were measured every 24 hours from uninduced cell cultures and induced cell cultures. DNAH10i uninduced cells entered a logarithmic phase, whereas DNAH10i induced cells grew slightly but maintained a similar titer throughout the 120 hours observed.

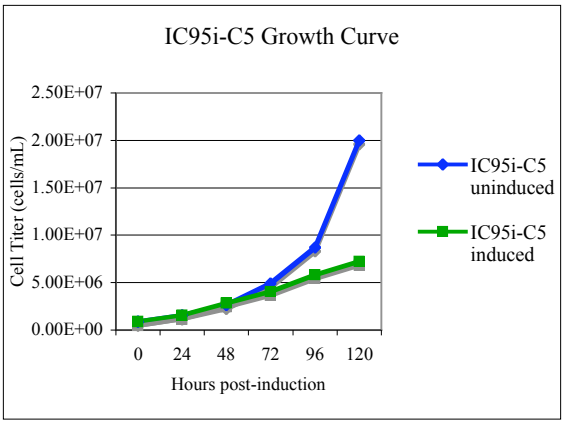

Figure 9 – IC95i-C5 growth curve. Cell titers were measured every 24 hours from uninduced cell cultures and induced cell cultures. IC95i-C5 uninduced cells entered a logarithmic phase, and IC95i-C5 induced cells grew at a linear rate. For the first few time points, the two cultures had roughly the same titer, but as the uninduced cells entered log phase, the difference between the two cultures became more clear.

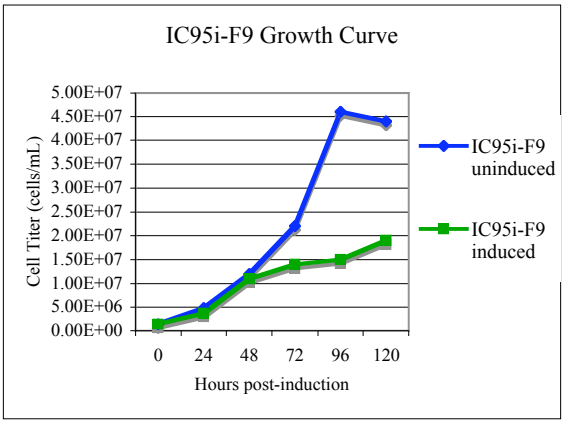

Figure 10 – IC95i-F9 growth curve. Cell titers were measured every 24 hours from uninduced cell cultures and induced cell cultures. Much like the IC95i-C5 cells, the IC95i-F9 uninduced cells grew logarithmically, and the induced cells grew at a more linear rate. The rate of IC95i-F9 growth surpassed that of both IC95i-C5 and DNAH10i, although the trends are still the same.

IC95i induced cells grew at a linear rate, and thus were able to maintain the same initial level of growth as the uninduced cells. After 72 hours, however, the logarithmic rate of the uninduced cells surpassed the linear rate of the induced

cells. A comparison between the strains can be found in Appendix A. Based on the similar growth rates of DNAH10 and IC95i-C5, all other experiments were conducted with the IC95i-C5 clonal line.

Sedimentation assays and time-lapse show marked motility defect in induced cells

Sedimentation assay graphs are shown in Figure 11 and Appendix B. Uninduced cells from both strains have very small optical density differences, less than 0.05 units. Induced cells have marked decreases in optical density, showing a motility defect in both strains. DNAH10 induced cells have a more constant density change over time, with a final difference of 0.35.

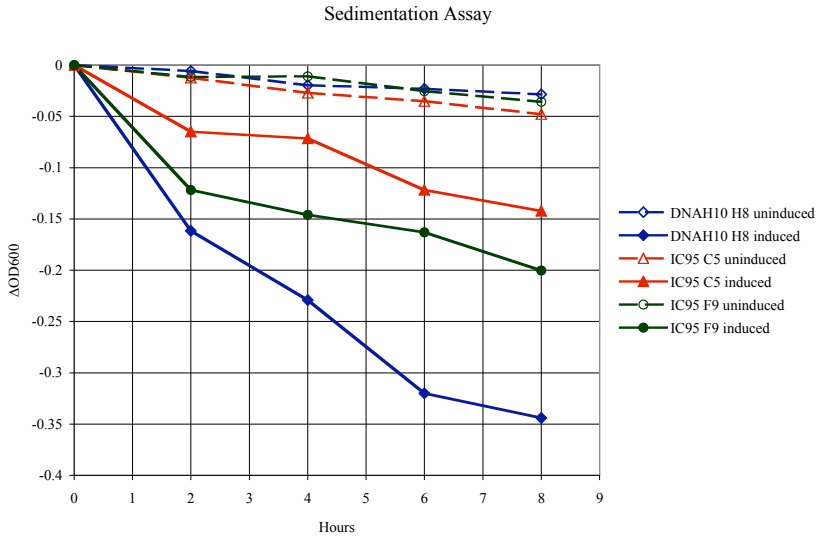

Figure 11 – Sedimentation assay for DNAH10i and IC95i. Optical density at 600nm was observed over a period of eight hours. Uninduced cells had no significant decrease in optical density. DNAH10i induced cells had a sharp and considerable decrease in optical density, and IC95i induced cells had a smaller but still significant decrease in optical density.

Such a sharp decrease in optical density suggests a severe motility defect. IC95i induced cells do not have as drastic a difference, with a smaller slope of decreasing density and a final difference of 0.15. These data suggest a moderate motility defect (slower growth and sluggish movement, as described in Baron et al, 2007) at this time point.

Time-lapse graphs from the uninduced and the 48-hour time point are shown for DNAH10i in Figure 12 and IC95i in Figure 13, and additional figures for other time points are in Appendix C. The time-lapse echoes the results of the sedimentation, where DNAH10i induced cells have 62% more immotile cells than the uninduced culture.

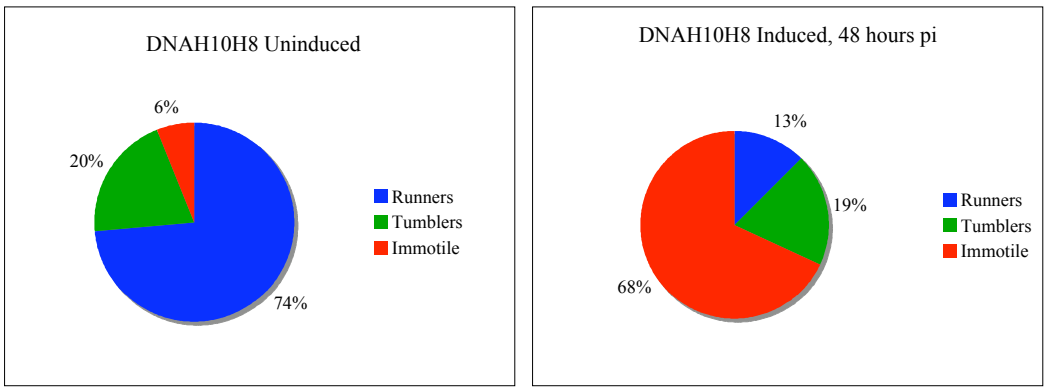

Figure 12 – Time-lapse data for DNAH10i. Cells were treated with tetracycline to induce RNAi knockdown, and uninduced and induced cells were characterized based on quality of movement over 30 second intervals. Induced cells here are cells that have been induced for 48 hours. A dramatic increase in the number of immotile cells can be clearly seen here, with a 62% difference between the two cultures.

A rise in immotile cells is also seen for IC95i, but again this difference is less dramatic than with DNAH10i, with 25% more immotile cells in the induced

sample. A larger number of cells in the IC95i culture started out as tumblers, but in each strain the percentage of tumbler cells remained the same.

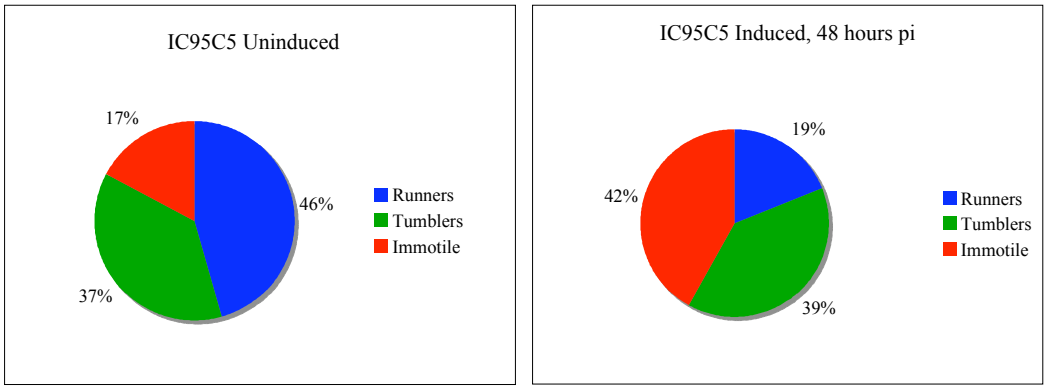

Figure 13 – Time-lapse data for IC95i-C5. Cells were treated with tetracycline to induce RNAi knockdown, and uninduced and induced cells were characterized based on quality of movement over 30 second intervals. Induced cells here are cells that have been induced for 48 hours. The 25% increase in immotile cells mirrors other data that suggest a moderate motility defect. The number of tumbler cells was larger to begin with, but no change was seen over time.

The rise in immotile cells in DNAH10i is gradual, shown in Figure 14. This result is in parallel with the growth curve data, where the difference in cell titer between uninduced and induced cells increases over time.

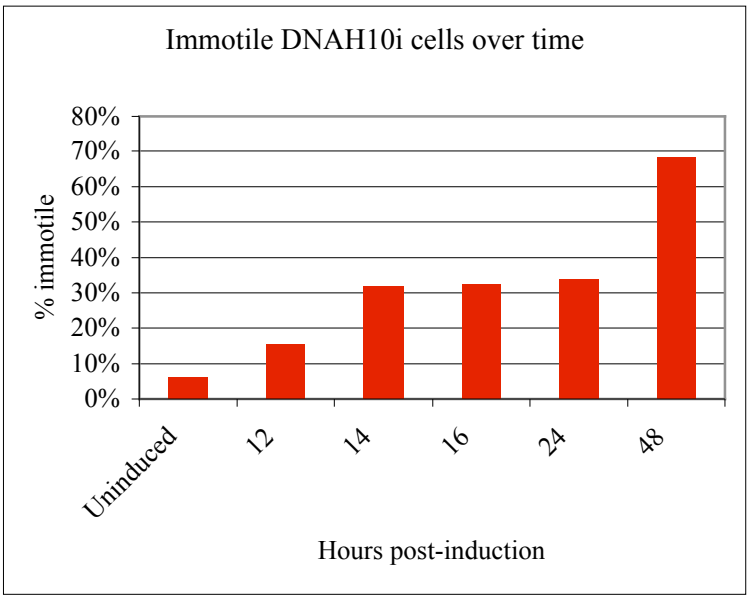

Figure 14 – Immotile DNAH10i cells over time. Numbers in this chart come from the time-lapse data over several timepoints post-induction with tetracycline. The increase in immotile cells is gradual and increases with small jumps over time, instead of one large sudden jump.

The same is not true for the rise in immotile IC95i cells, where a sudden change is seen at the 48 hour post-induction time point after relative stability.

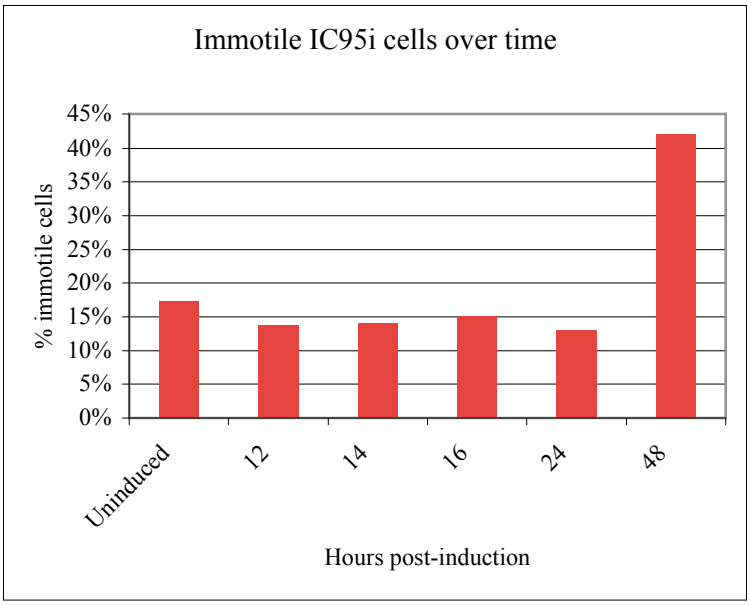

Figure 15 – Immotile IC95i cells over time. In contrast to the DNAH10i data, the number of immotile IC95i cells stayed more or less constant for the first 24 hours, with an increase at the 48 hours post-induction time point.

SEM shows deformed induced cells

Scanning electron microscopy revealed induced cells with marked deformities. A normal trypanosome is shown in Figure 16, and an example of the marked cellular deformities present is shown in Figure 17.

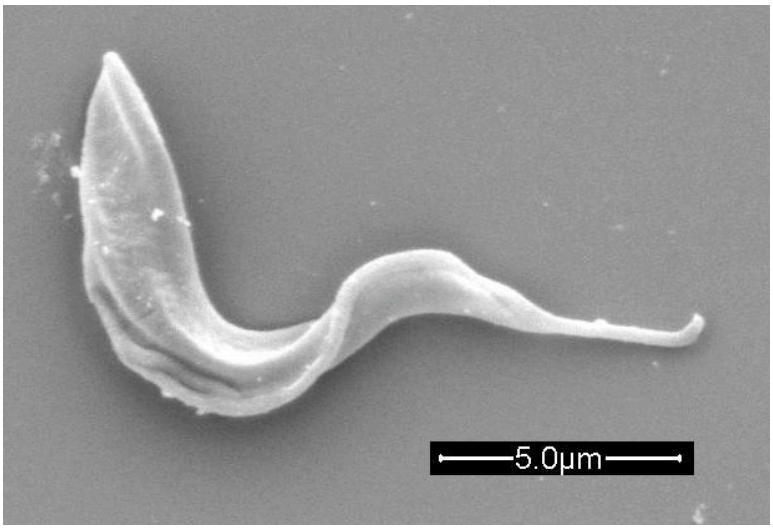

Figure 16 – SEM of uninduced DNAH10i. This trypanosome appears perfectly normal, with the flagellum attached to the cell body (anterior end at right of picture) and no obvious deformities present.

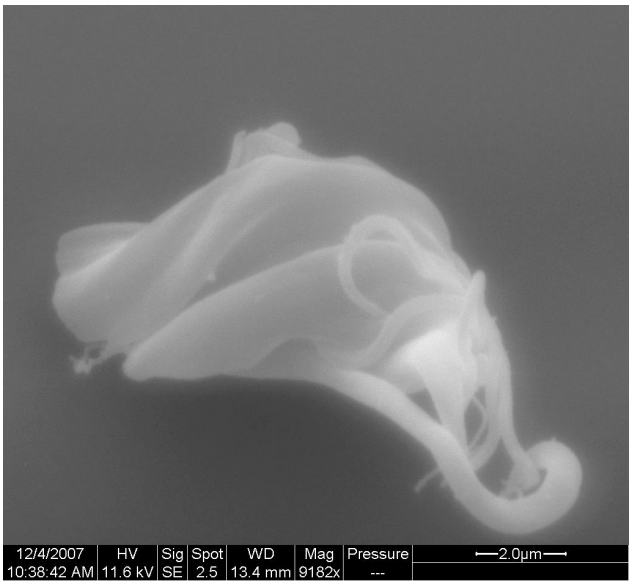

Figure 17 – SEM of deformed tet-induced DNAH10i cells. Here two or three cells are present, stuck to each other in such a way that it is difficult to ascertain where one cell ends and the next begins. Somewhere between two and four flagella are present along the center and bottom edge of the cells, and the flagella and cells themselves appear to have structural problems and interesting shapes. The overall integrity of these cells and the rest of the cells in the sample suggest a real phenotype as opposed to preparation artifacts.

For these cells the flagella are difficult to localize and the actual boundaries of the cells are nearly impossible to pinpoint. Not all induced cells are deformed in this way, but the cells that are would certainly have motility problems.

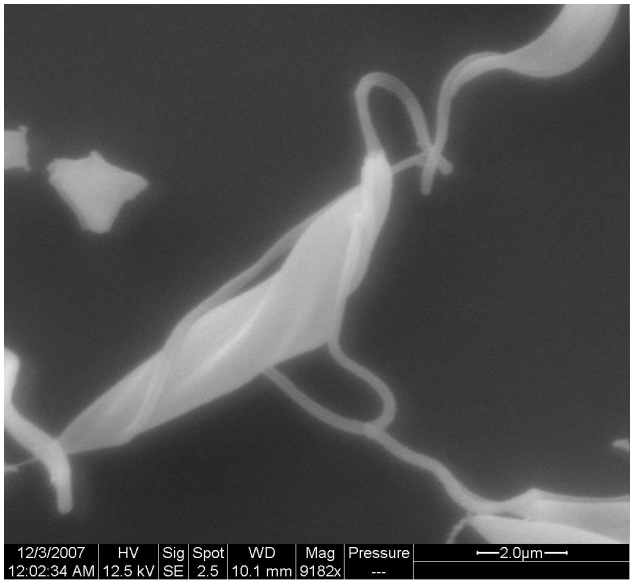

Figure 18 – SEM of multiple flagella on a tet-induced DNAH10i trypanosome. Flagellar division occurs before cellular division in trypanosomes. Usually only one division occurs at a time, so the presence of multiple flagella is indicative of a cellular division defect. Here a trypanosome has at least three flagella, with two flagella detached partially from the cell body.

Some cells appear to have multiple flagella attached to one large cell body, as shown in Figure 18, suggesting a problem in cytokinesis. Some flagella are partially detached from their cell bodies. Other cells appear to have achieved most of cytokinesis but are still clumped together (Figure 19), and it is difficult to determine how these cells are stuck together.

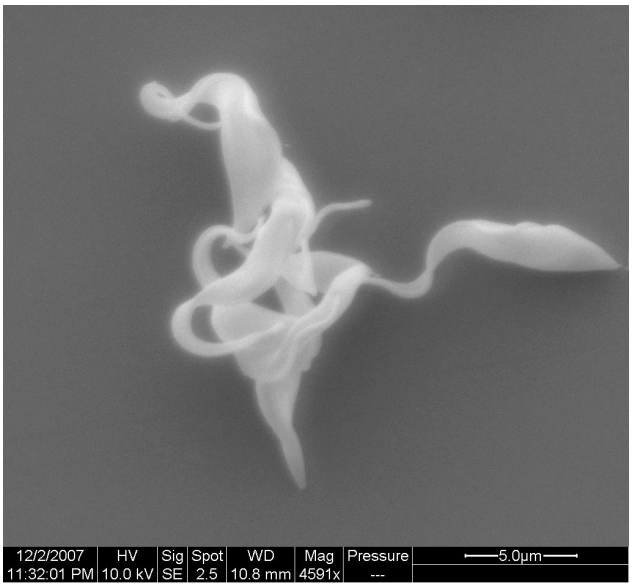

Figure 19 – SEM of tet-induced DNAH10i cluster. Improper flagellar movement can lead to incomplete cell division, which is shown in the cluster above. Four or five trypanosomes can be seen on the left, with one normal looking trypanosome on the right. These cells appear to have undergone most of cytokinesis but are stuck together. Clumps such as these were present in roughly 44% of all fields examined in the scanning electron microscope.

Similar results were present in the IC95i samples. An uninduced IC95i trypanosome is shown in Figure 20, while an unhealthy-looking induced trypanosome is shown in Figure 21.

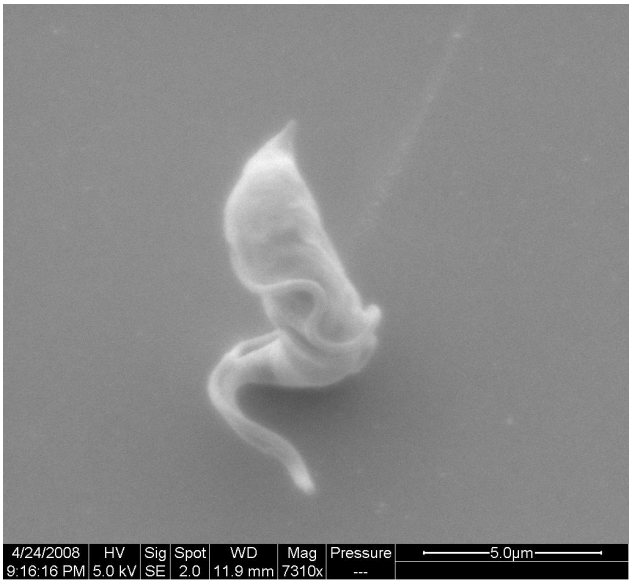

Figure 20 – SEM of uninduced IC95i. Uninduced IC95 cells looked normal, with regular cell shape and overall healthy appearance. In this image the flagellum is clearly visible, sinuously traveling down the side of the cell.

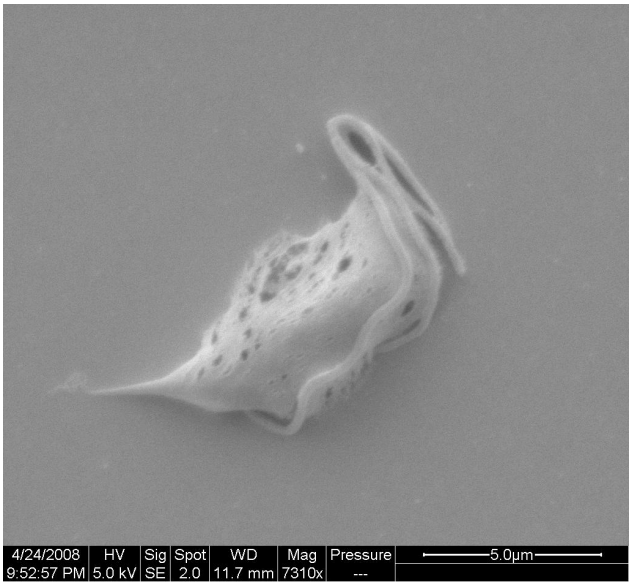

Figure 21 – SEM of tet-induced IC95i. This induced trypanosome has at least two flagella, which appear to be attached along most of the cell body. The cell body itself appears to be breaking or otherwise falling apart. This was not seen with many other induced cells, and may rather be a function of sample preparation than of effect of IC95 knockdown.

Visible cellular defects were less dramatic but more numerous in IC95i cells. Clumps like the one shown in Figure 19 were present in 37% of all fields examined in the scanning electron microscope. This data plus the raw counting data are found in Table 1.

Table 1 – Raw Data for SEM

DNAH10i	# Normal Cells	# Deformed Cells	Total Cells	% Deformed Cells
Induced	65	33	98	34%
Uninduced*	9	2	11	18%
IC95i				
Induced*	6	13	19	68%
Uninduced	25	4	29	14%
	Normal Fields	Fields w/Defects	Total	% Fields w/Defects
DNAH10i Un	39	11	50	22%
DNAH10i In	28	22	50	44%
IC95i Un	41	9	50	18%
IC95i In	31	19	50	37%

"Normal" describes a regular looking trypanosome that is free from obvious defect, and "Deformed" describes a trypanosome with a detached flagellum, multiple flagella present on a single cell body, multiple cells clumped together in such a way that they would not be able to be taken apart, or gross deformation of the cell body itself. Asterisks refer to samples that were low in density, resulting in overall low cell count.
"Normal fields" were fields of view that contained no trypanosomes with obvious cellular defects. "Fields w/defects" were fields of view that did contain trypanosomes with visible cellular defects.

Fluorescence and TEM

DAPI-staining images can be found in Figures 22-25. Figure 22 shows an uninduced DNAH10i sample, and Figure 23 shows the induced DNAH10i sample. In both samples, each cell appears to have the normal arrangement of one nucleus and one kinetoplast. Figures 24 and 25 show the IC95i uninduced and

induced samples respectively. The IC95i uninduced sample appears normal, just like the DNAH10i sample, but the IC95i induced sample shows cells with interesting nuclear structures. Many nuclei are present within one cell, and more than two kinetoplasts are present as well, indicating a replication of genetic material without division of the cell itself. Raw data from this experiment can be found in Table 2.

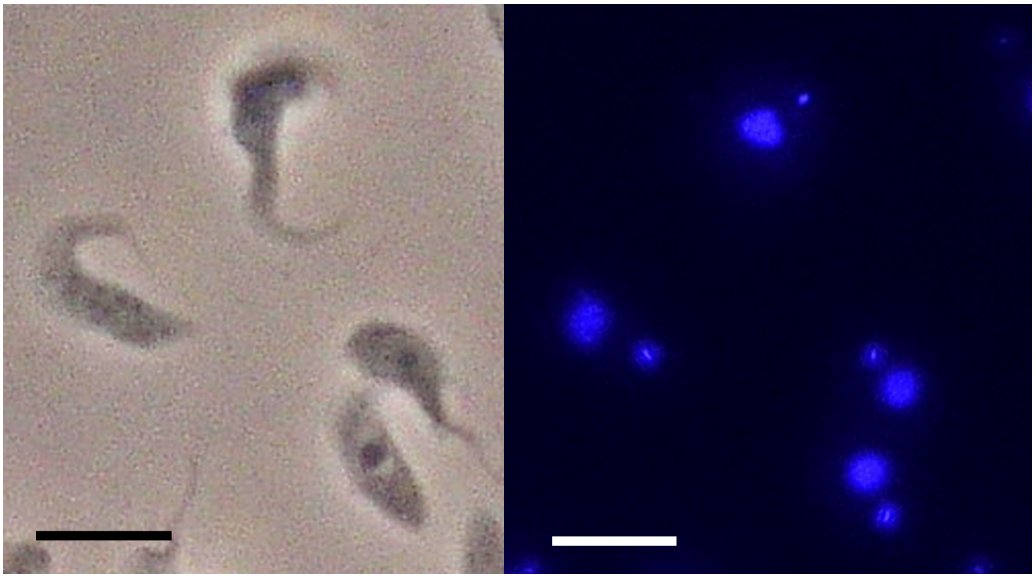

Figure 22 – DAPI of uninduced DNAH10i. These cells, induced for 48 hours, were attached to a poly-lysine slide, fixed in paraformaldehyde and stained with DAPI. Left image is phase-contrast, right is DAPI fluorescence. Each cell comes with two blue staining regions: the larger region is the nucleus, and the smaller more intense dot is the kinetoplast. These cells look normal with one kinetoplast and one nucleus per cell. Scale bars = 10μm.

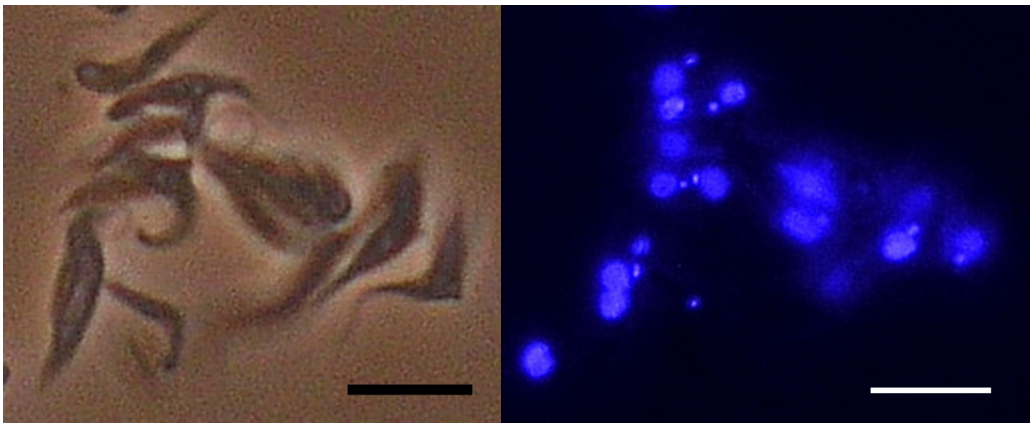

Figure 23 – DAPI of induced DNAH10i. These cells, induced for 48 hours, were attached to a poly-lysine slide, fixed in paraformaldehyde and stained with DAPI. Left image is phase-contrast, right is DAPI fluorescence. Here it is harder to see some of the kinetoplasts due to the number and orientation of the cells, although most cells appear normal. Scale bars = 10µm.

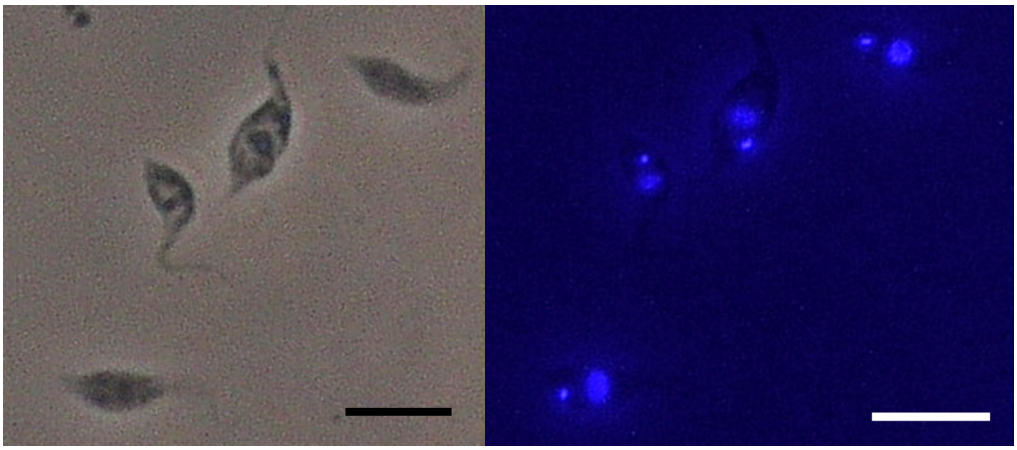

Figure 24 – DAPI of uninduced IC95i. These cells, induced for 48 hours, were attached to a poly-lysine slide, fixed in paraformaldehyde and stained with DAPI. Left image is phase-contrast, right is DAPI fluorescence. The second cell from the left has two kinetoplasts, which is present in early cell division, before the nucleus has replicated. Scale bars = 10µm.

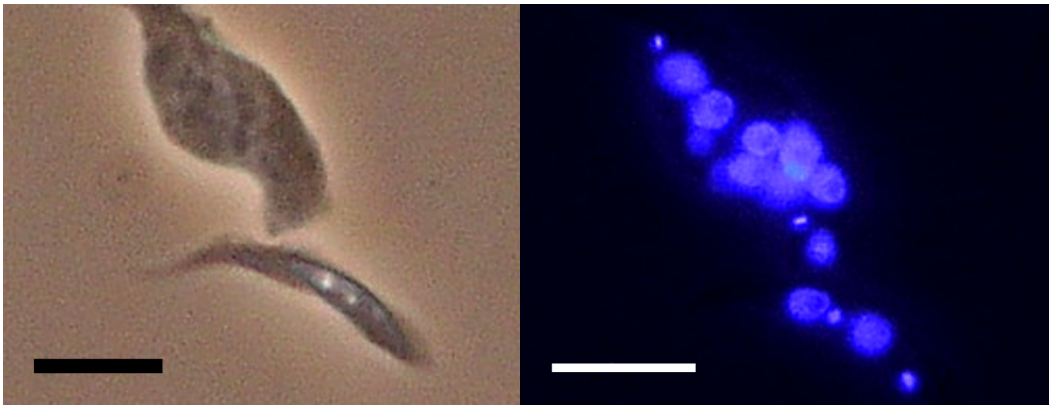

Figure 25 – DAPI of induced IC95i. These cells, induced for 48 hours, were attached to a poly-lysine slide, fixed in paraformaldehyde and stained with DAPI. Left image is phase-contrast, right is DAPI fluorescence. The top cell has eight to ten nuclei and at least two kinetoplasts. The bottom cell appears ready for cytokinesis, with two nuclei and two kinetoplasts that are in the proper orientation for cell division. Scale bars = 10µm.

Table 2 – Raw Data for DAPI

Cell Strain	DNAH10 Un	DNAH10 In	IC95 Un	IC95 In
Total cells	153	145	126	85
Abnormal cells	21	35	21	23
% abnormal	13.73%	24.14%	16.67%	27.06%
Cells DAPI off	10	12	11	13
% DAPI off	6.54%	8.28%	8.73%	15.29%

Numbers of abnormal cells as seen with fluorescence staining. "Abnormal" cells refers to cells that were visually deformed under phase microscopy, either with detached flagella or gross cell body defects. "DAPI off" refers to cells with more than one kinetoplast and/or nucleus.

Transmission electron microscopy images of DNAH10i axonemes are presented in Figures 26-27. Figure 26 shows an uninduced DNAH10i axoneme, and Figure 27 shows an induced DNAH10i axoneme. Unfortunately, it is difficult to make out details of the axonemal structures in either image. It is possible to see the radial spokes connecting the outer microtubules with the central pair, and the

rough outlines of the microtubules. The dynein arms are lost within a non-resolvable haze, but based solely on contrast, it appears that there are no substanial gaps or holes in the structure, suggesting that all proteins are present within the axoneme.

Figure 26 – TEM of uninduced DNAH10. Detergent-extracted axoneme from a DNAH10i uninduced cell. This micrograph shows the axoneme in the center surrounded by other cellular proteins. The outer ring and central pair of microtubules are present, as are the radial spokes connecting the two. The remains of the paraflagellar rod appear to be on the left of the axoneme. Other proteins withing the axoneme are not distinguishable, but do not appear to be absent. Scale bar = 200nm.

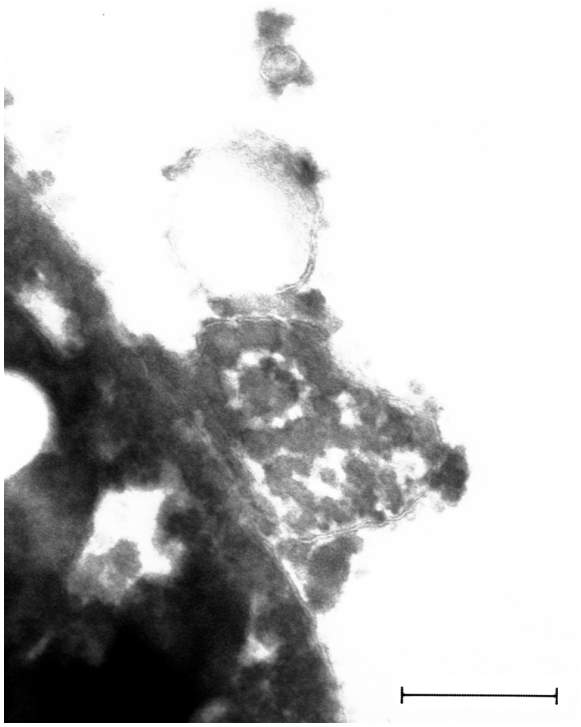

Figure 27 – TEM of induced DNAH10. Detergent-extracted axoneme from a DNAH10i induced cell. This micrograph shows the axoneme in the center surrounded by other cellular proteins. Bright circles in the image are holes in the nearby resin. The outer ring and central pair of microtubules are present, as are the radial spokes connecting the two. The remains of the paraflagellar rod appear to be on the lower right of the axoneme. Other proteins within the axoneme are not distinguishable, but do not appear to be absent. Scale bar = 200nm.

DISCUSSION:

Proper flagellar movement is required for cell division and motility of *T. brucei*. In addition, the proper assembly and placement of proteins in the dynein complex is needed for proper flagellar movement to occur. TbDNAH10 and TbIC95 encode for proteins that are required for proper flagellar motility, as evidenced in selective knockdowns of those genes.

Growth and Division Results Are Unique

Both proteins are needed for proper propagation of the cells. Induced DNAH10i cells suffered from a poor growth rate, essentially maintaining the same level of cell titer over the course of 120 hours. Induced IC95i cells grew better than the induced DNAH10i, but were unable to grow at the rate of the uninduced cells. The induced IC95i grew at a linear rate, showing a diminished ability to divide. Sedimentation assays showed a clear motility defect, with a serious defect present in DNAH10i and a moderate defect in IC95i.

The time-lapse data for DNAH10i suggest a gradual increase in the number of immotile cells. This gradual increase could be the result of all new daughter cells being affected by the lack of TbDNAH10, or from the recycling of dynein proteins. New flagella would be impacted more by the lack of TbDNAH10 than the already existing flagella. Rates of immotile cells would then increase as cells divided and as new flagella were made. This can be inferred from Figure 15, as the major increases in percentage of immotile cells take place

in roughly 18 hour intervals, an average doubling time for uninduced DNAH10i cells. IC95i does not share this particular trend in increasing immotile cells; in fact, the data shows a large jump after 24 hours post-induction. This can be explained as evidence that the phenotype present in induced IC95i is not as strong as the one in induced DNAH10i. Dividing cells in induced IC95i cultures that lack the protein are still able to swim and not be classified as immotile until the 48 hour time point. At this point, there are enough new cells with the defect that the phenotype begins to be seen at higher levels, and results in the apparent jump in immotility. When compared to TbDNAH10, TbIC95 has less of an impact on the overall motility of the flagellum and cell. It is still important, as IC95i induced cells show changes in motility, but the overall effect on the protein being knocked down is less.

When TbDNAH10 and TbIC95 mutants are compared to other flagellar mutants in *T. brucei*, many of the same general trends are seen: sedimentation assays show a motility defect and time-lapse analysis indicates an increase in the number of immotile and tumbler cells (Baron et al 2007b). However, all other procyclic flagellar mutants share similar growth of the cell lines between the uninduced and induced strains. TbDNAH10 and TbIC95 induced cells have a marked growth difference from the uninduced cells. While cell division defects have been demonstrated in the bloodstream form of *T. brucei*, they have not been seen in the procyclic form (Broadhead et al 2006). DNAH10i and IC95i induced

cells, which are procyclic, are showing a noticeable difference in overall growth from the uninduced.

Why do DNAH10i and IC95i mutants exhibit such a growth defect when other flagellar mutations do not? One explanation is that these proteins may have a role in regulation of flagellar beat to the extent that the flagellum is not able to move in a productive way. While the other mutants exhibit motility defects, the severity of the phenotype is roughly the same as IC95i, and are not quite as strong as the defect present in DNAH10i. IC95i has a better growth rate, as opposed to DNAH10i which has a very marked growth defect. It could be that this difference in motility is enough to provoke a growth defect.

This growth defect might also be a result of additional protein defects. The inner-arm dynein complex is large and involves many proteins; loss of a protein within the I1 complex may have a ripple effect on other proteins nearby, including the dynein regulatory complex, shown to be important for motility and division in the bloodstream form (Ralston et al 2006, Broadhead et al 2006). It was noticed that several of the mutants previously examined could be rescued by agitation on a shaker (Ralston et al 2006; Baron et al 2007); the same could not be said for DNAH10i (Appendix F). Ralston et al (2006) hypothesized that mutations with an indirect effect on flagellar motility would result in cellular distortion that could not be resolved by agitation. These knockdowns could be making other changes in the flagellum, and it could be these indirect changes that

result in the phenotype that is present. This could also explain why there is a difference between DNAH10i and IC95i. If the lack of each protein leads to different secondary effects, then the overall phenotype will be reflective of the different effects.

While the evidence clearly shows that these genes and their resulting protein products are required for proper motility of *T. brucei*, it has not been shown that these proteins are indeed localized to the inner-arm dyneins. It has been hypothesized that outer-arm dyneins are responsible for the formation of the initial beat of the flagellum; inner-arm dyneins, on the other hand, were hypothesized to be responsible for propagation of the wave down the length of the flagellum (Baron et al 2007; Dutcher 1995). This study supports this hypothesis, as induced trypanosomes were witnessed under light microscopy maintaining a flagellar beat but lacking movement of the cell body. If these proteins were a part of the outer-arm dyneins, then it would be expected that all flagellar movement would cease or greatly diminish as a direct result of loss of flagellar beat (Branche et al 2006). As a beat must be present in order for the rest of the flagellum to move, loss of the ability to form a beat would result in no movement of the flagellum. With the flagellar beat still present in DNAH10i and IC95i cells, it can be concluded that the outer-arm dyneins are still functioning and creating the beat.

IC95i Clones

Two different types of IC95i were examined - IC95i-C5 and IC95i-F9, referring to the wells in which each clone was brought up. Despite being the same cell line, F9 grew much faster than C5 (Appendix A). There were other differences present in the time-lapse data and the sedimentation assay; however F9 echoed C5 with magnitude and general trends in the data, suggesting that the TbIC95 knockout was leading to the phenotype seen in both strains, even if one was able to handle the defect better than the other. A hypothesis to explain this difference in the clones is the act of single-cell dilution itself. If the single cell in one of the wells had independently acquired a mutation, it would create a cell line that was not the same as the cell lines in the other wells. We are operating under the assumption that the clones are genetically identical or otherwise very similar to each other, and seeing the differences between two of the cell lines repudiates this idea. There is a possibility that the founding cell for the cell line had different levels of the RNAi inducing plasmid, which would then lead to different expression of the RNAi and thus a different phenotype. However, this is unlikely due to the similarities in sedimentation and time-lapse motility assays between C5 and F9. Because both lines behave in similar ways, it is more likely that the F9 line is simply able to grow at a faster rate due to a different genetic mutation. Since the two clones showed the same trends, C5 was chosen as a representative sample due to similarities in growth with DNAH10i.

SEM and Deformities

Images taken using scanning electron microscopy show the presence of a cell division defect, but it does not explain the defect. It is known that trypanosomes rely on properly functioning flagella to complete cytokinesis, and much of what is visible in these samples can be explained as an error in cytokinesis. Since SEM is only able to resolve details of the external features of the cell, it is impossible to identify division defects that may be occurring inside the cell. In addition, there are several artifacts from the fixation preparation of the sample that can distort the results, including rounded and dehydrated-looking cells. In the uninduced and induced samples of both DNAH10i and IC95i, some of the trypanosomes exhibit flagella that are partially detached from the cell body. Although the flagella appear more fully detached in the induced samples due to other cellular body defects, the frequency of detached flagella is the same for uninduced and induced samples. The trypanosome flagellum should be secured to the body of the cell through protein attachment, and the preparation should not be so harsh as to sever this attachment. Flagellar detachment has been seen in trypanin mutants (Ralston and Hill, 2006), so it is possible that changes within the flagellum will result in a difference in extracellular appearance. Trypanin is a part of the dynein regulatory complex (DRC), located in relative close proximity to the inner-arm dynein complex (Wirschell et al 2007). While the RNAi being used

should not impact the DRC directly, there may be an effect caused by structural changes in the nearby I1 complex.

These studies have proven intriguing, as the phenotypes seen with both defects are not those seen in *Chlamydomonas*. The DHC mutant in *Chlamydomonas* did not have such a dramatic cell division phenotype (Mysteral et al 1999), and the IC138 mutant had a more pronounced effect than the TbIC95 mutant (Hendrickson et al 2004). This could be due to the differences between the species resulting in a different severity of the mutation. The overall phenotype of a motility defect was observed in both species, but the severity of the phenotype was different. However, it has not been demonstrated that the genes used in these studies are the same as the ones used in the *Chlamydomonas* studies. Before any serious conclusions are drawn concerning the different phenotypes present between *Chlamydomonas* and *T. brucei*, it should be confirmed that the comparison is being made between the right proteins and not between completely unrelated proteins.

Inconclusive DAPI and TEM

DAPI staining and transmission electron microscopy results are currently inconclusive but hold promise for future experiments. Trypanosome cell division is closely linked with replication of the kinetoplast and basal body, where kinetoplast and subsequent basal body division occurs before nuclear division. Using DAPI, it is possible to determine number of nuclei and kinetoplasts in each

cell, thus determining stage in cell division at the time of staining. However, there are a few constraints, with the major constraint being the inability to differentiate between normal cells and mutated cells using the fluorescence staining alone. A number of the physiologically deformed cells are mitotically normal, and some cells with more than one kinetoplast are undergoing normal cell division. As a result, it is difficult to determine the difference between a mutated cell that would not have been able to undergo successful mitosis and a cell that was perfectly normal using DAPI alone. Many times the corresponding phase contrast image lacks the details required to determine if a cell would successfully undergo mitosis, or the cell has not yet taken on an externally visible phenotype. IC95i cells showed more of a difference between the uninduced and induced cells with the DAPI staining, although whether or not that is an actual difference remains to be seen. Cell division defects to this extent are usually only seen in the bloodstream form of *T. brucei*, (Broadhead et al 2006), which makes future studies of these genes of particular interest.

There has also been no evidence present in transmission electron microscopy images to show that any structural change occurs in the axoneme. This is interesting considering the strong phenotype observed with growth and motility. A number of more motile mutants have had visible structural changes when examined in transmission electron microscopy (Baron et al 2007; Branche et al 2006; Mysteral et al 1999; Ralston et al 2006). In addition, the number of

clean axonemes (where the 9 + 2 arrangement and most internal proteins can be seen) obtained using our TEM has been statistically insignificant. If more axonemes could be examined, we might notice a missing part of the inner-arm dynein or another associated protein.

Future Direction

Other future work should include a quantitative analysis on the induced IC95i RNA present in the cell to confirm gene knockdown, in the form of Northern blots or of qRT-PCR. There is a very good possibility that the lack of a phenotype is partially due to an incomplete knockdown of TbIC95. However, incomplete knockdowns often display a distinctive phenotype, so it is also possible that TbIC95 mutants will have more motility and growth than TbDNAH10 mutants. Future work to fully trace the location of the proposed proteins for these mutants would also be helpful, for it would provide confirmation of which protein is being affected by the knockdowns. Along the same lines, transfections with the genes being studied in *Chlamydomonas* would be interesting. A plasmid could be designed with a sequence to promote transcription of a replacement protein from *Chlamydomonas* (DHC I1-alpha or IC138), and this plasmid can be transfected into current DNAH10i or IC95i cells. If the two proteins are complementary, then the replacement protein should be able to behave like the native protein, bind in a similar manner to other proteins nearby, and recover from the RNAi knockdown. This would imply that the

replacement protein is able to interact appropriately with other native proteins in the flagellum. However, the replacement protein may not complement the knockdown simply because the replacement protein is from a completely different species. Incomplete recovery from the knockdown would also help to clarify the differences in the protein behavior between the two species, and could help explain why one phenotype is seen in one species and not the other.

The work presented here is an excellent starting point for many future studies, suggesting that the components of the inner-arm dynein are required for proper flagellar motility. With work to further elucidate the functions and behaviors of these dynein complexes, greater understanding of the mechanisms by which flagella operate can be achieved. This may lead to better treatments and drugs for African Sleeping Sickness, or extend further and lead to treatments of human ciliary and flagellar diseases.

APPENDIX

Appendix A: Supplemental Growth Curve Data

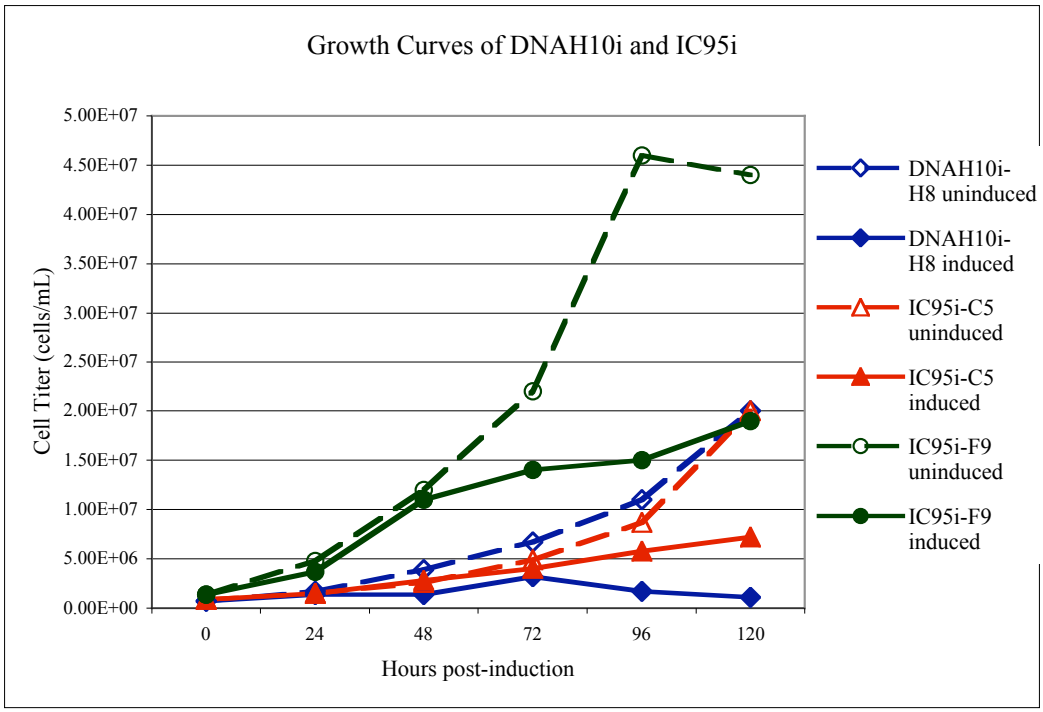

Full growth curve plot comparing uninduced and induced cultures across cell lines. Here it is possible to see that DNAH10i and IC95i-C5 have similar growth rates, while IC95i-F9 grows much faster. The same general trends are present between uninduced and induced cells, it is simply the magnitude of the change that is different.

Cell titers for the graph above

Hours	DNAH10H8 uninduced	DNAH10H8 induced	IC95C5 uninduced	IC95C5 induced	IC95F9 uninduced	IC95F9 induced
0	6.90E+05	6.90E+05	8.70E+05	8.70E+05	1.40E+06	1.40E+06
24	1.70E+06	1.40E+06	1.50E+06	1.50E+06	4.80E+06	3.70E+06
48	3.90E+06	1.40E+06	2.60E+06	2.80E+06	1.20E+07	1.10E+07
72	6.70E+06	3.20E+06	4.90E+06	4.00E+06	2.20E+07	1.40E+07
96	1.10E+07	1.70E+06	8.70E+06	5.80E+06	4.60E+07	1.50E+07
120	2.00E+07	1.10E+06	2.00E+07	7.20E+06	4.40E+07	1.90E+07

Appendix B: Supplemental Sedimentation Data

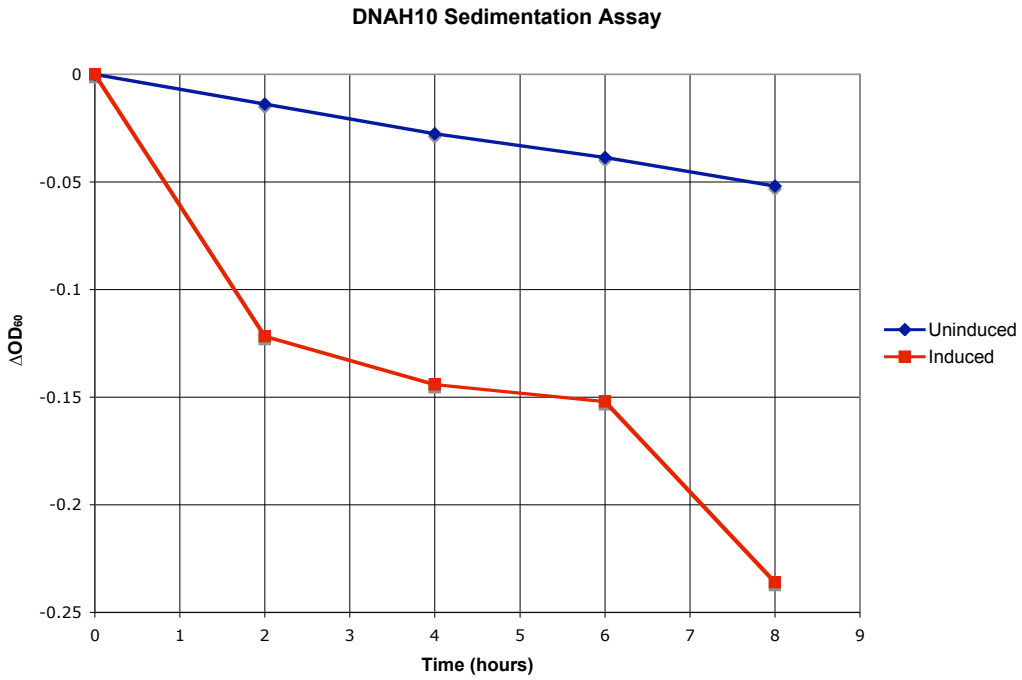

DNAH10 sedimentation assay conducted in July, 2007. Induced cells had a larger difference than the uninduced cells. The overall change here is not as severe as the most recent sedimentation assay, but the overall trend and change between uninduced and induced is the same.

Table for the sedimentation assay above.

	uninduced	uninduced shaken	induced	induced shaken
0	0.245	0.2463	0.3006	0.311
	0.2484	0.2492	0.3107	0.3172
2	0.251	0.2615	0.2181	0.3558
	0.2465	0.2636	0.2554	0.3613
4	0.2515	0.2808	0.2262	0.3672
	0.2587	0.2846	0.2287	0.3761
6	0.26	0.3004	0.1948	0.3909
	0.268	0.305	0.1847	0.2926
8	0.264	0.3192	0.1849	0.4047
	0.273	0.3215	0.1615	0.4136

Tables for the reported sedimentation assay in Figure 11.

DNAH10i	uninduced	uninduced shaken	induced	induced shaken
0	0.2427	0.235	0.36	0.3767
2	0.2408	0.2467	0.2902	0.4517
4	0.2402	0.2597	0.2685	0.4976
6	0.2455	0.2686	0.3001	0.6202
8	0.2645	0.2931	0.2357	0.5796

IC95i	uninduced	uninduced shaken	induced	induced shaken
0	0.2365	0.2352	0.3461	0.3545
2	0.2403	0.2528	0.3294	0.3943
4	0.241	0.2682	0.3356	0.4072
6	0.2566	0.2917	0.3194	0.4413
8	0.2738	0.3216	0.325	0.4674

Appendix C: Supplemental Time-Lapse Data

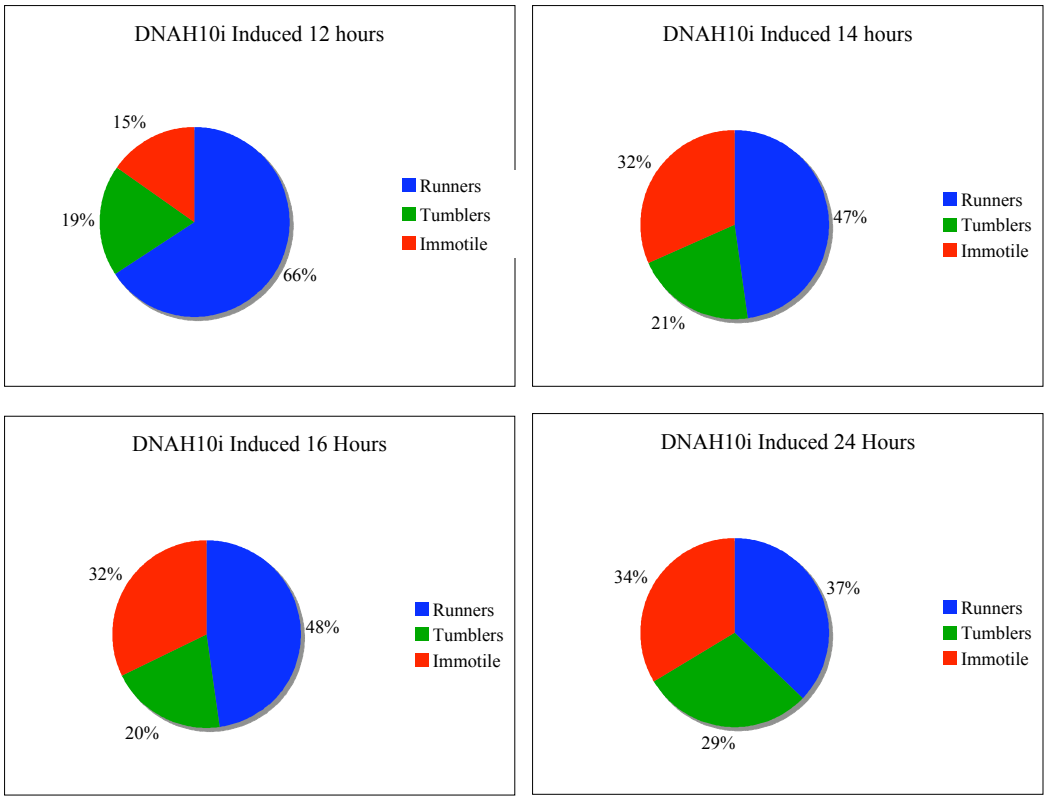

Additional time points for DNAH10i.

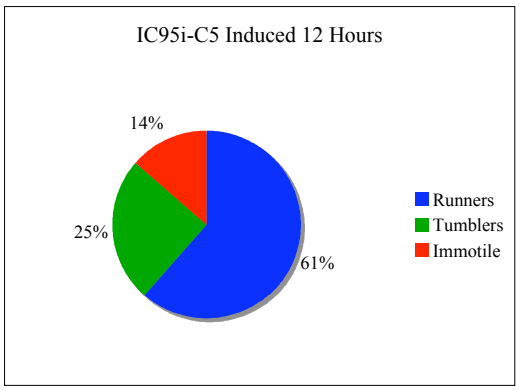

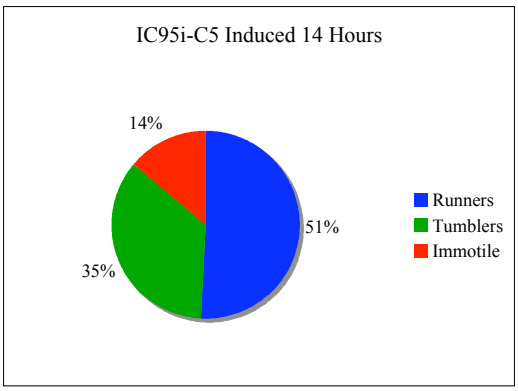

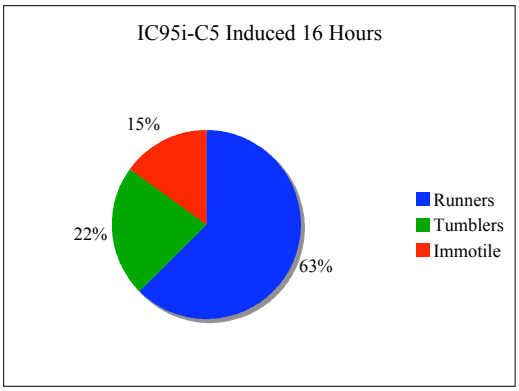

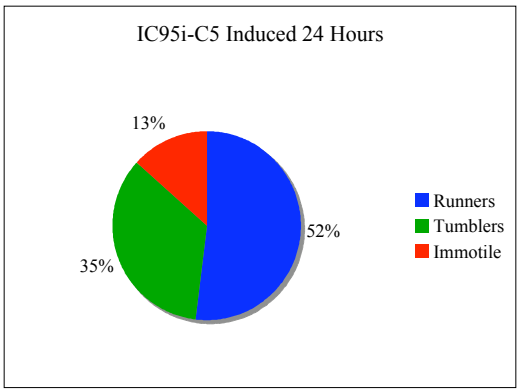

Additional time points for IC95i-C5.

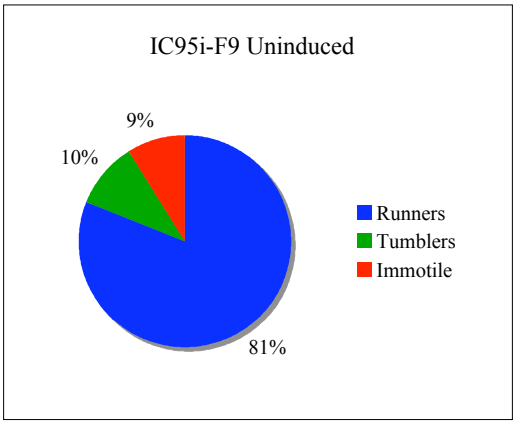

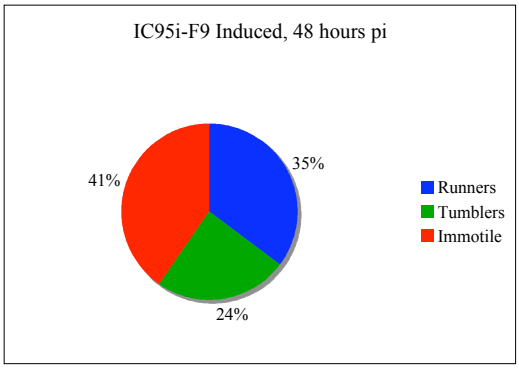

Main time points for IC95i-F9

Appendix D: Shaking Suppression Experiment

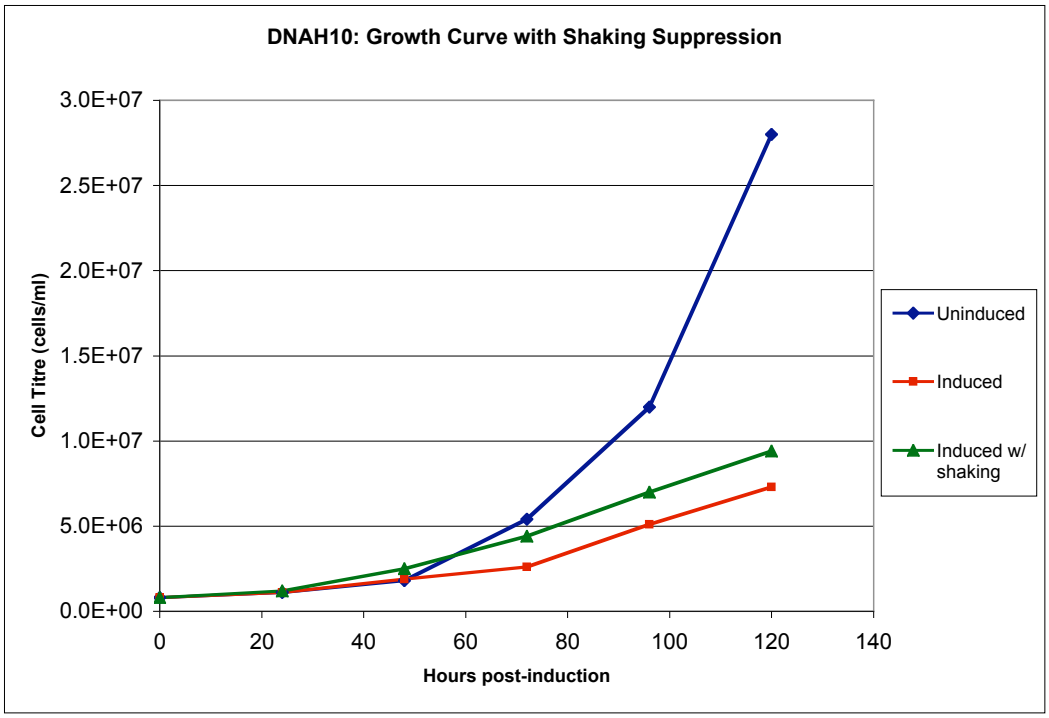

This was conducted over July, 2007. The induced culture that was grown on a shaker at 80rpm had little difference from the regular induced culture.

REFERENCES

Alberts, B., et al. 2002. *Molecular Biology of the Cell.* 4th ed. New York: Garland Science.

Baron, D. M., Z. P. Kabututu, and K. L. Hill. 2007. Stuck in reverse: loss of LC1 in *Trypanosoma brucei* disrupts outer dynein arms and leads to reverse flagellar beat and backward movement. *Journal of Cell Science* 120, 1513-1520.

Baron, D. M., K. S. Ralston, Z. P. Kabututu, and K. L. Hill. 2007. Functional genomics in *Trypanosoma brucei* identifies evolutionarily conserved components of motile flagella. *Journal of Cell Science* 120, 478-491.

Bastin, P., T. J. Pullen, F. F. Moreira-Leite, and K. Gull. 2000. Inside and outside of the trypanosome flagellum: a multifunctional organelle. *Microbes and Infection* 2, 1865-1874.

Bastin, P., T. J. Pullen, T. Sherwin, and K. Gull. 1999. Protein transport and flagellum assembly dynamics revealed by analysis of the paralysed trypanosome mutant *snl*-1. *Journal of Cell Science* 112, 3769-3777.

Branche, C., et al. 2006. Conserved and specific functions of axoneme components in trypanosome motility. *Journal of Cell Science* 119, 2442-2455.

Broadhead, R., et al. 2006. Flagellar motility is required for the viability of the bloodstream trypanosome. Nature 440, 224-227.

Burgess, S. A., and P. J. Knight. 2004. Is the dynein motor a winch? *Current Opinion in Structural Biology* 14, 138-146.

Centers for Disease Control. 2004. "West African trypanosomiasis Fact Sheet," Division of Parasitic Diseases, http://www.cdc.gov/Ncidod/dpd/parasites/trypanosomiasis/factsht_wa_trypanosomiasis.htm [accessed 4.30.08].

Chappuis, F., et al. 2005. Eflornithine Is Safer than Melarsoprol for the Treatment of Second-Stage *Trypanosoma brucei gambiense* Human African Trypanosomiasis. *Clinical Infectious Diseases* 41, 748-51.

Donelson, J. E. 2003. Antigenic variation and the African trypanosome genome. *Acta Tropica* 85, 391-404.

Dutcher, S. K. 1995. Flagellar assembly in two hundred and fifty easy-to-follow steps. *Trends in Genetics,* 11, no. 10:398-404.

Gadelha, C., B. Wickstead, and K. Gull. 2007. Flagellar and Ciliary Beating in Trypanosome Motility. *Cell Motility and the Cytoskeleton* 64, 629-643.

Gibbons, I. R. 1988. Dynein ATPases as Microtubule Motors. *Journal of Biological Chemistry* 263, 15837-15840.

Hendrickson, T. W., et al. 2004. IC138 is a WD-repeat dynein intermediate chain required for light chain assembly and regulation of flagellar bending. *Molecular Biology of the Cell* 15, no. 12:5431-5442.

Hill, K. L. 2003. Biology and Mechanism of Trypanosome Cell Motility. *Eukaryotic Cell* 2, no. 2:200-208.

Kennedy, P. G. E. 2004. Human African trypanosomiasis of the CNS: current issues and challenges. *Journal of Clinical Investigation* 113, no. 4:496-504.

Klingbeil, M. M., S. A. Motyka, P. T. Englund. 2002. Multiple Mitochondrial DNA Polymerases in *Trypanosoma brucei*. *Molecular Cell* 10, no. 1:175-186.

Mello, C. C., and D. Conte Jr. 2004. Revealing the world of RNA interference. *Nature* 431, 338-342.

Myster, S. H., et al. 1999. Domains in the 1-alpha Dynein Heavy Chain Required for Inner Arm Assembly and Flagellar Motility in *Chlamydomonas*. *Journal of Cell Biology* 146, 801-818.

Nicastro, D., et al. 2006. The Molecular Architecture of Axonemes Revealed by Cyroelectron Tomography. *Science* 313, 944-948.

Pearce, L. 1921. Studies on the Treatment of Human Trypanosomiasis with Tryparsamide (the Sodium Salt of N-phenylglycineamide-*p*-arsonic acid). *Journal of Experimental Medicine* 34, no. 6 Supplement no. 1:1-104.

Pullen, T. J., M. L. Ginger, S. J. Gaskell, and K. Gull. 2004. Protein targeting of an unusual, evolutionary conserved adenylate kinase to a eukaryotic flagellum. *Molecular Biology of the Cell* 15, 3257-3265.

Ralston, K. S., and K. L. Hill. 2006. Trypanin, a component of the flagellar dynein regulatory complex, is essential in bloodstream form African trypanosomes. *Public Library of Science Pathogens* 2, no. 9:873-882.

Ralston, K. S., A. G. Lerner, D. R. Diener, and K. L. Hill. 2006. Flagellar Motility Contributes to Cytokinesis in *Trypanosoma brucei* and Is Modulated by an Evolutionarily Conserved Dynein Regulatory System. *Eukaryotic Cell* 5, no. 4:696-711.

Stich, A., P. M. Abel, S. Krishna. 2002. Human African trypanosomiasis. *BMJ* 325, 203-206.

Vaughan, S., and K. Gull. 2003. The trypanosome flagellum. *Journal of Cell Science* 116, 757-759.

Wirschell, M., T. Hendrickson, W. S. Sale. 2007. Keeping an Eye on I1: I1 Dynein as a Model for Flagellar Dynein Assembly and Regulation. *Cell Motility and the Cytoskeleton* 64, 569-579.

Woehlke, G., and M. Schliwa. 2000. Walking on two heads: the many talents of kinesin. *Nature Reviews: Molecular Cell Biology* 1, 50-58.

World Health Organization. 2006. "African trypanosomiasis (sleeping sickness) Fact Sheet," WHO Media Center, http://www.who.int/mediacentre/factsheets/fs259/en/ [accessed 4.30.08].